Immunoglobulin somatic hypermutation in a defined biochemical system recapitulates affinity maturation and permits antibody optimization

Soo Lim Jeong[1], Hongyu Zhang[1], Shanni Yamaki[1], Chenyu Yang[1], David D. McKemy[1], Michael R. Lieber [ID][1,2]**, Phuong Pham** [ID][1] **and Myron F. Goodman** [ID][1,3,*]

[1]Department of Biological Sciences, University of Southern California, Los Angeles, CA 90089, USA, [2]Departments of Pathology, Biochemistry & Molecular Biology, and Molecular Microbiology & Immunology, Norris Comprehensive Cancer Center, University of Southern California Keck School of Medicine, Los Angeles, CA 90033, USA and [3]Department of Chemistry, University of Southern California, Los Angeles, CA 90089, USA

ABSTRACT

We describe a purified biochemical system to produce monoclonal antibodies (Abs) *in vitro* using activation-induced deoxycytidine deaminase (AID) and DNA polymerase η (Polη) to diversify immunoglobulin variable gene (IgV) libraries within a phage display format. AID and Polη function during B-cell affinity maturation by catalyzing somatic hypermutation (SHM) of immunoglobulin variable genes (IgV) to generate high-affinity Abs. The IgV mutational motif specificities observed *in vivo* are conserved *in vitro*. IgV mutations occurred in antibody complementarity determining regions (CDRs) and less frequently in framework (FW) regions. A unique feature of our system is the use of AID and Polη to perform repetitive affinity maturation on libraries reconstructed from a preceding selection step. We have obtained scFv Abs against human glucagon-like peptide-1 receptor (GLP-1R), a target in the treatment of type 2 diabetes, and VHH nanobodies targeting Fatty Acid Amide Hydrolase (FAAH), involved in chronic pain, and artemin, a neurotropic factor that regulates cold pain. A round of *in vitro* affinity maturation typically resulted in a 2- to 4-fold enhancement in Ab-Ag binding, demonstrating the utility of the system. We tested one of the affinity matured nanobodies and found that it reduced injury-induced cold pain in a mouse model.

INTRODUCTION

Antibody surface display technologies (1) have permitted robust and effective methods to implement stringent selections for proteins expressed on the surface of ribosome (2),

bacteriophage (3), yeast (4) or mammalian cells (5) that bind to a wide variety of ligand molecules. Target ligands may be present free in solution or attached to external surfaces such as cell membranes (6). A widespread application of surface display is aimed at the selection of monoclonal antibodies (MAbs), as described in numerous review articles (7). The display technologies have been widely implemented for MAb selection because libraries with a high complexity can be generated efficiently and can be rapidly screened against a target antigen (Ag) by panning or cell sorting (8).

For the successful development of therapeutic Abs, achieving high affinity and specificity toward a target Ag is essential to increase efficacy and to minimize potential side effects. In mammals, the generation of Abs with high affinity toward Ags occurs in activated B-cells through mutagenic diversification of variable (V) regions of immunoglobulin (Ig) genes, a process known as IgV somatic hypermutation (SHM) (9,10). SHM requires activation-induced deoxycytidine deaminase (AID) (11), which deaminates cytosine (C→U) preferentially at WRC (W = A/T, R = A/G) motifs (12–15) within the variable (V) region during active transcription of Ig genes. C→U deaminations in IgV regions occur at a rate $\sim 10^{-3}$–10^{-4}/bp/cell division, which is a million times higher than the average rate of somatic mutations (16,17). The U can be copied by correct incorporation of A opposite U resulting in a C→T transition mutation at the site of AID deamination (10). Alternatively, the G:U mismatches can undergo error-prone nucleotide excision repair or base excision repair. The two repair processes are error-prone because a low fidelity DNA polymerase, e.g. Polη, is used to fill in the long mismatch repair tract or short base excision repair tract, resulting in transition and transversion mutations occurring within the repair gaps (10). Polη tends to preferentially mutate 5′WA hot motifs (18). Human IgV sequences have evolved to enrich for WRC

hot motifs in the three Complementarity Determining Regions (CDR), which form the antigen binding pocket of Abs (19). AID's preferential deaminations of WRC hot motifs *in vitro* (12,20–22) and *in vivo* in CDR regions of IgV (23,24), ensure the mutagenic diversity of Ab paratopes in B-cells during the immune response. Numerous protein engineering strategies have been used previously for *in vitro* affinity maturation of Abs in surface display platforms. These included random mutagenesis of V regions of heavy (V_H) and light chains (V_L) through error-prone PCR or mutator bacterial strains (25–27) saturated or selected mutagenesis targeting only the Ag-binding CDR of V_H and V_L regions (28). However, this approach to diversify IgV genes often produces an excess of non-productive Ab variants that are not produced in human B-cells and may not be tolerated by the human immune system. In this paper, we describe a new method for generating MAbs, one which operates within a phage display platform to perform enzymatic affinity maturation in a test tube using AID and Polη.

This is the first example in which AID and Polη have been used in a purified biochemical system, making this the first biochemical reconstitution of the mutation phase of the Ig somatic hypermutation process. To serve as a proof-of-principle 'jumping-off' point, we have used our 'affinity maturation in a purified biochemical system' in two types of phage display libraries, one involving single chain variable fragment (scFv) Abs (29), a second using llama VHH nanobodies (30). Previously, we have shown that AID-catalyzed dC deamination spectra on ssDNA (22) and on a human Pol II transcribed IgV-gene agree with human B-cell SHM spectra at G/C sites (21). Here, we have used biochemically purified AID and Polη to try to more fully recapitulate the Ig affinity maturation spectrum of mutations at both G/C and A/T sites in IgV, similar to those occurring during affinity maturation in B-cells. But the most important and unique application of this technique is that it provides a way to increase Ab–Ag binding affinities by using a reiterative series of *in vitro* affinity maturation steps, first by purifying Abs selected during a phage display round and then by constructing a new AID-Polη diversified library that includes the initially selected Ab sequence, treated again with AID and Polη, for use in the next phage display selection round. The successive steps in library construction, AID-Polη induced mutation, Ab purification, new library construction, etc., are intended to approximately simulate what takes place during affinity maturation in B-cells. Applying *in vitro* mutagenesis by AID and Polη, we have developed a methodology to diversify naïve human scFv and VHH phage display libraries. Using AID and Polη-diversified libraries and iterative affinity maturation, we have isolated antibodies targeting three specific antigens: scFv antibodies against human glucagon-like peptide-1 receptor (GLP1-R), a target in the treatment of type 2 diabetes; VHH nanobodies targeting Fatty Acid Amide Hydrolase (FAAH), a membrane enzyme involved in chronic pain, and VHH nanobodies against artemin, a neurotropic factor involved the modulation of cold sensation in mammals. We tested one of the affinity matured artemin VHH Abs in a mouse model to determine its efficacy in relieving injury-induced cold pain in comparison with a commercially available full-length Ab. We sequenced each of the affinity matured Abs to determine whether the AID-Polη generated mutations were localized in IgV complementary determining regions (CDR) as previously reported (21,22), or in framework regions (FW). Therefore, our biochemical system recapitulates the Ig affinity maturation process in a manner that could have many important applications.

MATERIALS AND METHODS

Materials

M13mp2 phage and *Escherichia coli* CSH50 and MC1061 *ung*- strains are from our lab collection. pADL20c phagemid vector, *E. coli* TG1 strain were purchased from Antibody Design Labs (San Diego, CA). f3TR1 phage display vector and *E. coli* strain K91BK (31) were obtained from George P. Smith (University of Missouri, Columbia, MO). Naïve VHH library was purchased from Abcore, Inc. (Ramona, CA). VHH repertoire in this library was prepared from Peripheral Blood Mononuclear cells derived from 24 non-immunized Llamas and cloned into pADL20c phagemid vector. Purified recombinant mouse artemin protein (Ala112-Gly224 fragment) was purchased as lyophilized powder from R&D Systems, Inc., was reconstituted at 100 µg/ml in 4 mM HCl and stored at −20°C. Live cultures of *Sf9* cells expressing a recombinant human His_6-tagged glucagon-like peptide-1 receptor (GLP-1R) and biomass for purification (32) were obtained from Professor Raymond Stevens' lab (Bridge Institute, University of Southern California, CA). Recombinant GLP-1R protein was purified as described (32).

Human AID and Polη purification

Sf9 expressed GST-tagged AID was purified as described (12,13). AIDv(Δ15) was purified as described (33). N-terminal His-tagged full-length human Polη was expressed in *E. coli*. Collected cells (∼25 g) were resuspended in 180 ml of lysis buffer (50 mM Tris pH 7.5; 500 mM NaCl, 20 mM Imidazole, 10% glycerol, 10 mM 2-mercaptoethanol and four tablets of complete protease inhibitor (Roche) and lysed by French press. After centrifugation at 20 000 × g for 45 min, the supernatant was incubated with 7.5 ml Ni-NTA resin (Qiagen) for 30 min at 4°C on a rotating platform for 30 min. The NTA resin was washed with 50 ml of wash buffer 1 (50 mM Tris pH 7.5; 1 M NaCl, 20 mM Imidazole, 10% glycerol, 10 mM 2-mercaptoethanol) followed by 50 ml of wash buffer 2 (10 mM Na-phosphate pH 7.7, 500 mM NaCl, 20 mM imidazole, 10% glycerol, 10 mM 2-mercaptoethanol). His-tagged Polη was eluted with elution buffer (10 mM sodium phosphate pH 7.7, 500 mM NaCl, 200 mM imidazole, 10% glycerol, 10 mM 2-mercaptoethanol). Polη fractions were pooled and applied to a Superdex G200 26/60 gel-filtration column (GE Healthcare) using running buffer (20 mM Tris pH 7.5; 500 mM NaCl, 1 mM EDTA, 1 mM DTT, 5% glycerol). Peak fractions containing monomeric His_6-tagged Polη were collected and diluted with 4 volumes of a dilution buffer (20 mM sodium phosphate pH 7.3, 10% glycerol, 1 mM DTT). The diluted pool was loaded into a 1 ml mono S ion-exchange column equilibrated with Buffer A (20 mM Na-

phosphate pH 7.3; 100 mM NaCl, 10% glycerol, 10 mM 2-mercaptoethanol). After washing the column with 20 ml buffer A, his-Polη was eluted using 20 ml gradient of 100 ml NaCl to 1000 mM NaCl in buffer A. Pure His_6-Polη fractions were pooled, dialyzed overnight in a dialysis buffer (20 mM Tris, pH 7.5; 50 mM NaCl, 1 mM EDTA, 1 mM DTT, 10% glycerol) and stored at −70 °C.

Human FAAH purification

Human fatty acid amide hydrolase, FAAH (accession AH007340.2) was expressed and purified as follow. FAAH sequence corresponding to amino acids 30–579 (without the N-terminal transmembrane domain) was cloned into pMALx expression vector and expressed in *E. coli* CSH50 cells at 18°C overnight as MBP-tag fusion protein. The cells were harvested by centrifugation and washed once with 10 mM Tris pH 8.5 + 1 M NaCl. The pellet was resuspended in lysis buffer 20 mM Tris pH 8.5, 0.1% Triton X-100, 5 mM DTT, 1 M NaCl, 1 mM PMSF and lysed by sonication. After centrifugation at 20 000 × g for 30 min, the supernatant was incubated with Amylose resin (New England Biolabs). MBP-FAAH fusion protein was eluted with 40 mM Maltose and further purified by gel filtration using Superdex 200 gel filtration column (GE Healthcare). To purify untagged FAAH, the MBP tag was cleaved with Factor Xa Protease for 3 h in buffer containing 20 mM Tris–HCl pH 8.5, 100 mM NaCl, 2 mM $CaCl_2$. Untagged FAAH protein was further cleaned by gel filtration. MBP-FAAH and FAAH proteins were stored in 20 mM Tris–HCl pH 8.5, 1M NaCl and 5% glycerol at −80°C.

Diversification of IGHV3-23*01 gene *in vitro* by human AID and Polη

Close circular DNA gapped substrates with the *lacZα-IGHV3-23*01* region as ssDNA were constructed as described previously (22). AID deamination reactions (30 μl total volume), containing GST-AID (100 ng), RNase (100 ng) and a gapped DNA substrate (500 ng) dissolved in a reaction buffer (10 mM Tris–HCl, pH 8.0, 1 mM EDTA, 1 mM dithiothreitol), were carried out at 37°C for 5 min and terminated by twice extracting the DNA product with phenol:chlorophorm:isoamyl alcohol (25:24:1). The deaminated gapped DNA (1 μg) were subjected to Polη gap-filling synthesis at 37°C for 2 h in a tube (100 μl total volume) containing 40 mM Tris–HCl (pH 8.0), 50 mM NaCl, 2.5% glycerol, 10 mM dithiothreitol, 2.5 mM $MgCl_2$, 500 μM each of the four dNTPs and 300 ng of human Polη. Synthesis reaction was terminated and Polη was removed by twice extracting the DNA product with phenol:chlorophorm:isoamyl alcohol (25:24:1). AID and Polη treated DNA were desalted 4 times with H_2O using Amicon Ultra-0.5 10 kDa (Millipore) centrifugal filter unit.

Analysis of AID and Pol η-induced mutations in IGHV3-23*01 sequence *in vitro*

50 ng of desalted DNA were incubated with 50 μl of uracil glycosylase deficient (*ung⁻*) MC1061 competent cells and transformation was carried out by electroporation using a BioRad electroporator. Following addition of 1 ml of SOC medium and incubation at 37°C for 30 min, aliquots of electroporated cells (5–200 μl) were added to a tube containing 3 ml of soft agar (7.5 g of bacto-agar in 1 l of H_2O; autoclave and keep at 42°C), 250 μl of mid-log CSH50 α-complementation host cells, 50 μl of 5-bromo-4-chloro-3-indolyl-beta-D-galactopyranoside (X-gal, 50 mg/ml), 50 μl of Isopropyl β-D-1-thiogalactopyranoside (IPTG, 100 mM), mixed and poured on the top of a minimal medium plate. After plate incubation overnight at 37°C, wild-type (colorless) and mutant (light or dark blue) M13 phage plaques were counted. DNAs from mutant M13 phages were isolated and the entire *IGHV3-23*01* region was sequenced by standard Sanger sequencing.

Construction of a mini synthetic scFv library

Synthetic human genes, V_H (18 genes) and V_L (20 genes) were synthesized by Integrated DNA Technologies IDT (Coralville, Iowa). Each V_H gene contains a portion of (G4S)4 linker sequence: GGTGGTGGTGGTTCTG-GTGGTGGTGGTTCTGGCGGCGGCGGCTCC at the 3′ end, and each V_L gene contains a portion of (G4S)4 linker sequence: GGCGGCGGCGGCTCCGGTGGTG-GTGGATCC at the 5′ end. V gene fragments also contain a BglI restriction site for cloning into pADL20c phagemid vector. Random fusion of V_H to V_L via a flexible (G4S)4 linker was carried out using overlapping PCR. PCR reaction (50 μl volume) was assembled with 5 ng of V_H + V_L gene pool, 100 ng each of VH-F (TACTCGCG-GCCCAGCCGGCCA) and VL-R (TGG TGT TGG CCT CCC GGG CCA) primer, and 25 μl of 2× PCR master mix (Promega). After 25 cycles of PCR (94°C – 1 min; 94°C – 30 s, 55°C – 30 s, 72°C – 1 min for 25 cycles; 72°C for 2 min), scFv PCR products were purified, digested with BglI (New England Biolabs) and ligated with dephosphory-lated BglI-digested pADL-20c vector using T4 DNA ligase. Ligated DNA were transformed into *E. coli* TG1 cells and plated on LB plates with 0.2% glucose and ampicillin (100 μg/ml). After incubation overnight at 37°C, TG1 transformant colonies were harvested, resuspended in LB medium in the presence of 15% glycerol and stored at −80°C.

Phagemid scFv 'double gap' construction

To make the scFv double-gap constructions, dsDNA phagemid pADL-20c and pADL20-scFv library were first digested with BglI and PvuI restriction enzymes, respectively. Linearized dsDNAs were cleaned and purified by QI-Aquick PCR purification kit (Qiagen). Linear pADL20c and pADL20-scFv (0.5 μg each in 45 μl of H_2O) were heat denatured at 70°C for 5 min in separate PCR tubes and combined. After addition of 10 ul of 20× SSC buffer (3 M NaCl, 300 mM Sodium citrate, pH 7.0), the mixture was incubated at 60°C for 5 min and placed on ice. Double gapped DNA from eight tubes were pooled, desalted three times with H_2O using Amicon Ultra-0.5 10 kDa (Millipore) centrifugal filter unit and stored in 1 mM Tris (pH 8.0) and 0.1 mM EDTA at −20°C. To verify the efficiency of gap formation, 10 pg of each linear pADL20c, pADL20-scFv, and the

double gap constructs were used to transform 50 µl of TG1 electrocompetent cells by electroporation. The transformation mixtures were plated on LB plates in the presence of 100 µg/ml of ampicillin and TG1 bacterial colonies were counted after incubation at 37°C overnight.

AID and Polη mutagenesis for scFv double-gap constructs

To maximize the scFv diversity, the gapped constructs were incubated with AID in a series of individual tubes for different incubation times (30 s, 45 s, 1 min, 2 min, 5 min, 10 min, 20 min and 30 min). Each AID deamination tube (30 µl total volume), contains 500 ng of scFv double gap constructs, GST-AID (100 ng), RNase (100 ng) in a reaction buffer (10 mM Tris–HCl, pH 8.0, 1mM EDTA, 1 mM dithiothreitol) at 37°C. At the indicated time point for each tube (30 s, 45 s, 1 min, 2 min, 5 min, 10 min, 20 min or 30 min), AID deamination was stopped by twice extracting the reaction mixture with phenol:chlorophorm:isoamyl alcohol (25:24:1). Deaminated scFv DNAs were combined and purified by QIAquick PCR purification kit (Qiagen). The deaminated scFv double-gap DNA (1 µg) were subjected to in Polη gap-filling synthesis at 37°C for 2 h in a tube (100 µl total volume) containing 40 mM Tris–HCl (pH 8.0), 50 mM NaCl, 2.5% glycerol, 10 mM dithiothreitol, 2.5 mM MgCl$_2$, 500 µM each of the four dNTPs and 300 ng of human Polη. Synthesis reaction was terminated and Polη was removed by twice extracting the DNA product with phenol:chlorophorm:isoamyl alcohol (25:24:1). AID and Polη treated DNA were desalted 4 times with H$_2$O using Amicon Ultra-0.5 10 kDa (Millipore) centrifugal filter unit and stored in 1 mM Tris (pH 8.0), 0.1 mM EDTA at −20°C. To analyze AID and Polη actions on the scFv sequence, the purified double gap constructs were used to transform 50 µl of TG1 electrocompetent cells by electroporation. The transformation mixtures were plated on LB plates in the presence of 100 µg/ml of ampicillin and incubated at 37°C overnight. pADL20-scFv phagemid from individual transformants were isolated and scFv regions were sequenced by Sanger sequencing. Sequence alignment and mutation analysis were performed using Sequencher program (Gene Code Corp.).

cDNA preparation

Tonsils collected from tonsillectomy of seven individuals were frozen in liquid nitrogen and pulverized using pestle and mortar. Total RNA were extracted using TRIzol reagent (ThermoFisher Scientific) according to the manufacturer protocol. ProtoScript II First Strand cDNA synthesis kit (New England Biolabs, MA) was used for cDNA preparation. 16 PCR tubes (40 µl volume each), containing 15 µg of RNA and the random primer mix (oligo-dT18 and random hexamers, 6 µM) was denatured at 65°C for 5 min and placed on ice. After addition of the ProtoScript reaction mix and enzyme mix, cDNA synthesis was carried out by incubation at 25°C for 5 min followed by 42°C for 60 min and enzyme inactivation at 80°C for 5 min. cDNA were pooled and stored at −70°C.

PCR Amplification of variable regions of Ab heavy chains (V$_H$) and light chain (V$_L$) repertoire

In order to reduce amplification bias, first PCR amplification was carried out in independent PCR tubes to amplify individual V gene segments, using all possible combinations with V$_H$ and V$_L$ forward and reverse primers. The primer sequences, allowing amplification of the entire repertoire of human antibody genes ([34](#)) are listed in Supplementary Table S1. Each PCR reaction (50 µl volume) was carried out in the presence of 375 ng of cDNA, 100 ng of each forward and reverse primers and 25 µl of 2× PCR master mix (Promega Corp.) using following PCR program: 94°C – 2 min; 94°C – 1 min, 55°C – 1 min, 72°C – 2 min for 30 cycles; 72°C for 10 min. PCR products were separated by 1.2% TAE agarose gel electrophoresis and PCR bands corresponding to V genes were cut out (VH: ∼380 bp, kappa/lambda: ∼650 bp), purified by QIAquick Gel Extraction Kit (Qiagen) and eluted in 10 mM Tris, pH 8.5. PCR products from each subfamily (V$_H$, kappa, lambda) were pooled separately and stored at –20°C.

The second round of PCR introduced BglI restriction sites at the 5′-end of V$_H$ and at the 3′-end of V$_k$ and V$_l$ genes. Reverse primers for V$_H$ and forward primers for V$_k$ and V$_l$ also contain additional sequences to form a flexible (G$_4$S)$_4$ linker between V$_H$ and V$_L$ to constitute scFv. The primers for second PCR amplification are listed in Supplementary Table S2. PCR reactions (50 µl volume) were set up for all pair of forward and reverse primers in the presence of 10–20 ng of a purified PCR product from the first PCR, 100 ng of each forward and reverse primers and 25 µl of 2× PCR master mix (Promega Corp.). PCR program is as follow: 94°C – 1 min; 94°C – 30 s, 55°C – 30 s, 72°C – 1 min for 25 cycles; 72°C for 5 min. The second PCR amplification produced single V$_H$ or V$_L$ product bands (∼430–450 bp), which were combined for each subfamily and purified by Qiaquick PCR purification kit (Qiagen).

scFv diversification by AID and Polη

V$_H$, V$_k$ and V$_l$ PCR products were mixed together at molar ratios of 2 V$_H$:1 V$_k$:1 V$_l$ to constitute a V gene mixture. AID deamination was carried out in a series of PCR tubes using a thermocycler. Each tube, containing 200 ng of the V gene mix in H$_2$O (50 µl volume) was heat-denatured at 94°C for 2 min and quickly cooled down to 37°C, followed by an immediate addition of GST-AID (100 ng). After incubation at 37°C for predetermined time (30 s, 45 s, 1 min, 2 min, 5 min, 10 min or 20 min), AID deamination was stopped by twice extracting the reaction mixture with phenol:chlorophorm:isoamyl alcohol (25:24:1). Deaminated V gene DNAs were combined, desalted three times with H$_2$O and concentrated using Amicon Ultra-0.5 10 kDa centrifugal filter unit (Millipore).

Polη error-prone synthesis was performed as follows. A PCR tube (50 µl total volume), containing 50–100 ng of the V gene mix (AID-treated or non-AID treated), 10 ng of a forward and reverse primers (scFv-F: TACTCGCGGCC-CACGCGGCCA, scFv-R: TGGTGTTGGCCTCAGCG-GCACT) in reaction buffer 40 mM Tris–HCl (pH 8.0), 50 mM NaCl, 2.5% glycerol, 10 mM dithiothreitol, 2.5 mM

$MgCl_2$ and 500 μM each of the four dNTPs was heat denatured and cool to 4°C to allow the annealing of the primers to V genes. Since the 3′-end of V_H and the 5-end of V_k/V_l PCR products contain a complementary sequences (GGC GGC GGC GGC TCC), annealed top strands of V_H and bottom strands of V_k/V_l can also serve as primers for Polη extension. DNA synthesis was initiated by addition of 300 ng of purified human Polη and incubated for 2 h at 37°C. Synthesis reaction was terminated and Polη was removed by twice extracting the reaction mixture with phenol:chlorophorm:isoamyl alcohol (25:24:1). Polη-treated DNAs from 20 to 24 tubes were combined, desalted 4 times with H_2O using Amicon Ultra-0.5 10 kDa centrifugal filter unit (Millipore) and stored in 1 mM Tris (pH 8.0), 0.1 mM EDTA at −20°C.

Generation of scFv repertoire by overlapping PCR

V genes treated with both AID and Polη was combined with V genes treated with AID alone and V genes treated with Polη alone and non-treated V genes at an equal concentration to use as templates to generate mutagenized scFv repertoire. The 3′-end of V_H and the 5-end of V_k/V_l contain complementary sequences allowing a fusion of V_H and V_L and forming a (G4S)4 linker for scFv by overlapping PCR. 96 PCR tubes (50 μl volume), each contains 10 ng of the V gene mixture, 100 ng of a forward primer (scFv-F: TACTCGCG-GCCCACGCGGCCA), 100 ng of reverse primer (scFv-R: TGGTGTTGGCCTCAGCGGCACT) and 25 μl of 2× PCR master mix (Promega) were subjected to 30 cycles of PCR: 94°C – 1 min; 94°C – 30 s, 55°C – 30 s, 72°C – 1 min for 30 cycles; 72°C for 2 min. Overlapping PCR produced a single PCR product (~850–900 bp) corresponding to scFv composition V_H-$(G4S)_4$-V_L. PCR products were combined, extracted twice with phenol:chlorophorm:isoamyl alcohol (25:24:1) and ethanol precipitated. The mutagenized scFv gene repertoire was resuspended in 10 mM Tris (pH 8.5) and stored at −20°C.

Cloning of scFv into f3TR1 phage display vector and generation of f3TR1-scFv phage display library

The mutagenized scFv gene repertoire and f3TR1 vector dsDNA were digested with BglI (New England Biolabs) for 3 h at 37°C. Digested scFv DNA were purified using QIAquick PCR purification kit (Qiagen) and eluted in 10 mM Tris (pH 8.5). The digested f3TR1 was de-phosphorylated with Shrimp Alkaline Phosphatase (New England Biolabs), purified using a Qiagen-tip 500 column (Qiagen) and resuspended in 10 mM Tris (pH 8.5). Ligation of scFv into f3TR1 vector was carried out at 16°C for 16 h by T4 DNA ligase (New England Biolabs) using scFv : f3TR1 molar ratio of ~2:1. Ligated DNAs were desalted four times with H_2O and concentrated using Amicon Ultra-15 10 kDa centrifugal unit (Millipore) and stored at −20°C.

The ligated DNAs were electroporated into *E. coli* competent cells MC1061 using Bio-Rad electroporator. To generate the mutagenized scFv library, a total of 240 electroporation was carried out. Aliquots (10–200 μl) of transformants were plated immediately on LB plates containing tetracycline (20 μg/ml) to determine the number of independent transformants in the library. To examine the quality of the library, random transformants were picked and scFv was sequenced using Sanger sequencing. V_H and V_L chains of sequenced scFv clones were identified and analyzed using IgBLAST tool (www.ncbi.nlm.nih.gov/igblast).

Purification of primary f3TR1-scFv phage library

Flasks with transformants in 2x YT medium were incubated at 37°C for 16 h to allow the production of primary f3TR1-scFv phages. The culture supernatants (total of 12 L) were collected after centrifugation and phages were precipitated by adding 15% volume of PEG/NaCl solution (16.6% PEG 8000 MW, 3.3 M NaCl) for 4 h at 4°C. Precipitated phages were harvested by centrifugation at 10 000 × g for 20 min. The phage pellets were resuspended in TBS buffer (1/30 volume of supernatant) and subjected to a second round of PEG/NaCl precipitation. Phage pellet from the second precipitation was resuspended in TBS buffer and 50% glycerol (typically 1 ml for each liter of supernatant) and stored at −20°C.

Preparation of high-titer phage stocks for bio-panning

K91BK cells were grown in 1 L flask containing 500 ml of 2×YT at 37 °C until OD_{600} of 1/10 dilution is 0.2 (~2.5 × 10^{12} cells) and infected with primary scFv phage (7.5 × 10^{11} TU). The flask was incubated without shaking for 15 min and six 90 ml each of the culture were distributed to six flasks each contains 1 L of prewarmed 2×YT medium supplemented with 0.22 μg/ml tetracycline (six flasks total). After shaking at 37°C for 35 min, tetracycline was added to a final concentration of (20 μg/ml), and phage production was continued for 16 h. A high titer human scFv phage library stock (5 × 10^{12} TU/ml) was harvested and purified as described above.

Generation and preparation of mutagenized Llama f3TR1-VHH phage library

Llama VHH repertoire was PCR amplified from Abcore's naïve VHH library using a forward (TATTACTCGCGGC-CCACGCGGCCATGGCT) and a reverse (GGTGATG-GTGTTGGCCCCAGGGGCTGAGGAGACGGTGAC) primers, which incorporate BglI restriction sites for cloning into f3TR1. VHH repertoire PCR products were subjected to AID and Pol η diversification using procedures described for the mutagenized human scFv library. 160 transformations by electroporation were carried out to obtain a mutagenized Llama VHH library (2.8 × 10^8 independent clones). A high titer VHH phage library stock (1.9 × 10^{13} TU/ml) was prepared for bio-panning.

Selection of phage antibody library by Bio-panning

Enrichment of phage particles displaying specific human scFv or Llama VHH were performed on MaxiSorp Nunc-Immunotubes. Protein antigens (3–10 μg/ml) in 1 ml of phosphate-buffered saline (PBS, pH 7.4) (50 mM Sodium bicarbonate pH 9.6 in case of artemin) were coated on the tube surface overnight at 4°C. After blocking with 2% (w/v)

skimmed milk powder in PBS (MPBS) for 1–2 h, an aliquot of phage library (f3TR1-scFv or f3TR1-VHH) containing 1×10^{12} phage TU was added to the tube in the first round of panning. For the subsequent rounds of panning, less phages (2×10^{11} TU) were used. After gentle rocking for 2 h at room temperature. Non-bound phages were eliminated by washing 10–15 times with PBS containing 0.1% Tween 20 (PBS-T), followed by two times washing with PBS. The bound phages were eluted by incubation with 1 ml of 10 µg/ml trypsin in PBS for 30 min at room temperature. Amplification of eluted phages was carried out by incubating 0.5 ml of eluted phage with 25 ml of exponentially growing *E. coli* K91BK cells in 2xYT medium without shaking for 30 min at 37°C. 75 ml of 2×YT medium supplemented with tetracycline (0.22 µg/ml) was added and the culture was transferred to a 37°C shaker (200 rpm). After 45 min, tetracycline was added to 20 µg/ml and phage production was continued for 16 h. Titers of eluted phage binders and amplified phage preps for each panning were determined by serial dilution and infection of K91BK cells as described for phage library titration.

For selection of GLP-1R specific Abs, *Sf9* cells expressing GLP-1R (32) was used as the target antigen. *Sf9* cell panning was carried out at 4°C, scFv phage (1×10^{12} TU) was pre-incubated with 2×10^7 control *Sf9* cells in PBS + 2.5% BSA for 1–2 h to deplete non-specific binding phages. 1×10^7 GLP-1R expressing cells were blocked in PBS + 2.5% BSA for 1 h and incubated with depleted phages for 1 h. Ice cold PBS was used for washing (10 times) by centrifugation at $300 \times g$ for 5 min. Bound phages were eluted by resuspending cells in 500 µl of PBS containing 10 µg/ml trypsin and incubate at RT for 30 min.

Screening for antigen-specific clones by phage ELISA

Individual K91BK colonies on titration plates from the last panning were pick into 96-deep well plates containing 1.5 ml of 2×YT + 20 µg/ml tetracycline and grown overnight in a shaker at 37°C to produce scFv or VHH phage particles. Phages from 1 ml of supernatant were precipitated with 150 µl of the PEG/NaCl solution and resuspended in 200 µl of PBS.

Each well of Nunc Maxisorp 96-well microplates was coated with 100 µl of 5–10 µg/ml of each antigen. After overnight incubation at 4°C, plates were blocked with 2% MPBS for 1.5 h followed by three washed with PBS-T and three washes with PBS. All washings were performed on AquaMax 2000 plate washer (Molecular Devices, LLC). The selected phage preparation was diluted 1:2 in 4% MPBS before adding 100 µl into each well, and incubated for 1.5 h. The plates were washed three times with PBS-T, followed by three times with PBS, and incubated with 100 µl of a 1:4000 dilution of anti-M13-HRP (Sino Biological US, Inc., Wayne, PA) in 2% MPBS for 1 h. Plates were washed 4 times with PBS-T and four times with PBS. TMB substrate solution 100 µl (Thermo Fisher Scientific) was added to each well (for 2–30 min). After adding 100 µl of 2 M sulfuric acid stop solution, the absorbance was read at 450 nm, using SpectraMax iD5 microplate reader (Molecular Devices, LLC).

Expression and purification of soluble scFv and VHH Abs

Coding sequences for antigen-specific scFv and VHH Abs were subcloned into the BglI sites of pADL-20c phagemid vector. The constructs were transformed into *E. coli* CSH50 cells and Abs were expressed as His$_6$-tagged soluble proteins in the periplasm. Cells were grown at 37°C in LB + 0.2% glucose + ampicillin (100 µg/ml). When the culture OD$_{600}$ reaches ∼0.7, IPTG (1 mM) was added to induce scFv/VHH expression at 30°C overnight. Cells from 1 L culture were harvested by centrifugation, resuspended in 400 ml ice-cold wash buffer (30 mM Tris pH 8.0 and 20% glucose and EDTA was added to 1 mM. After incubation at 4°C for 10 min, cells were spun down at 8000 × g for 20 min. The pellet was resuspended in 400 ml of ice cold 5 mM MgSO$_4$ and incubated for 10–15 min at 4°C. The supernatant containing a soluble scFv/VHH protein was collected by centrifugation at 8000 × g for 20 min. His$_6$-tagged scFv/VHH proteins were purified by affinity chromatography using 2–3 ml of Ni-NTA resin (Qiagen) using PBS as a wash buffer and eluted in PBS containing 300 mM Imidazole. In some cases, scFv/VHH were further purified by gel filtration using Superdex 75 column (GE Healthcare). Proteins were concentrated using Amicon Ultra-15 10 kDa centrifugal filter unit (Millipore) and stored in PBS at −70°C.

Titration ELISA

Titration ELISA was used to measure binding of purified scFv to GLP-1R. GLP-1R immobilization in a 96-well plate and blocking was carried out as described for phage ELISA. A purified scFv was prepared at varying concentrations (from 1 nM to 3 µM) in 2% MPBS. 100 µl scFv aliquot of each concentration was added to a well and incubated at room temperature for 1.5 h. The plate was then washed with TPBS and PBS three times each. Primary anti His-tag Mouse mAb (Cell signaling Technology, Inc.) was diluted 1:250 in 2% MPBS and added into each well. After 1.5 h incubation, wells were washed and secondary anti-mouse (goat-anti mouse-HRP; Santa Cruz Biotechnology) diluted 1:1000 in 2% MPBS was added and incubated for 1 h. After washing, TMB substrate solution was added for color development (15 to 30 min) and 2M sulfuric acid was added to stop the reaction. The absorbance was read at 450 nm, using SpectraMax iD5 microplate reader (Molecular Devices, LLC). The dissociation constant K$_D$ was calculated according to a published protocol (35).

Surface plasmon resonance (SPR)

Binding of purified VHH nanobodies to Artemin and to untagged FAAH proteins was determined using Biacore T100 instrument (GE Healthcare). Either the target antigen or individual VHH nanobody was suspended in 10 mM sodium acetate (pH 4.5) and immobilized on a CM5 Series S sensor chip (GE Healthcare) at 150–250 RU (response unit) using amine coupling chemistry according to the manufacturer's protocol (GE Healthcare). VHH Abs or target antigen at a concentration ranging from 10 to 500 nM in flow buffer (PBS–0.005% Tween) was injected onto the flow cells (flow rate 30 ml/min) for 120 s. The sensor chip surface was regenerated using 4 mM NaOH or 7 mM NaOH. Kinetic

constants for binding interaction were determined by fitting the sensorgrams with 1:1 binding model using Biacore T100 evaluation software, version 2.0 (GE Healthcare).

Cold plantar assay on mice

Inflammatory cold allodynia was induced in male and female wildtype mice (on the C57/Bl6 background; Jackson Labs) by a unilateral intraplantar hind paw injection of Complete Freund's adjuvant (CFA; 20 μl; Sigma) with behavioral tests performed two-days post-injection. The cold sensitivity of the hind paws of mice injected with purified llama-VHH and MAB1085 positive control (R&D Systems) was measured in the McKemy lab (Department of Biological Sciences, Neuroscience, University of Southern California, CA) using the previously described protocol (36,37). Mice were allowed to acclimate in Plexiglas chambers for 2 h prior to cold plantar testing performed on a glass surface held at 30°C. A compressed powdered dry ice pellet was then applied to bottom of the glass surface underneath the tested hind paw and withdrawal latencies (in seconds) were recorded for a total of three trials per paw for each time point. All experiments were approved by the University of Southern California Institutional Animal Care and Use Committee and performed in accordance with the recommendations of the International Association for the Study of Pain and Guide for the Care and Use of Laboratory Animals by the NIH (38).

Antibody administration into mice

Commercial anti-artemin antibody (MAB1085; Rat IgG2A; R&D Systems) and LM52-VHH nanobody was dissolved in saline and injected subcutaneously (s.c.) to the scruff at a concentration of 10 mg/kg body weight. Antibodies were injected on day 2 post-CFA. Responses were measured 1, 2, 4, 8 and 12 h post-antibody injection. All results from behavioral assays were expressed as mean ± SEMs for each group, as well as experimental numbers, as indicated in the text and figure legends. Behavioral data were analyzed by two-way repeated measures of ANOVA, followed by post-hoc Bonferroni analysis with the criterion for statistical significance was $P < 0.05$.

RESULTS

**Combined mutation spectrum of purified human AID and Polη acting on a human V gene IGVH3-23*01**

As a first step towards exploring the application of AID and Pol η in IgV affinity maturation in a defined biochemical system, we have examined their combined mutagenic action on a human *IGHV3-23*01*. This gene has frequently been used as an *in vivo* SHM reporter gene to identify mutations generated by AID and Polη that have occurred during normal immune response (39) and in chronic lymphocytic leukemia (40). We have used *IGHV3-23*01* as an *in vitro* target for AID and Polη and have determined their combined mutational spectrum (Figure 1). The substrate for AID and Polη was constructed by insertion of the IgV target downstream of *lacZ* within a single-stranded gapped

region M13mp2 bacteriophage (22). Incubation of the ssDNA gapped region was performed initially with AID (5 min at 37 °C) to catalyze the conversion of C to U, favoring deaminations in WRC target motifs (12,20,22,41), followed by incubation with Polη (2 h at 37 °C) to fill in the gap. Polη catalyzes base substitutions at a frequency of ∼1%, typically within W:A and G:T target motifs (18,42) while accurately incorporating A opposite virtually all of the AID-generated U sites. Following transfection into *E. coli*, DNA was sequenced from *lacZ* mutant phage (clear and light blue plaques). AID-catalyzed deaminations of dC to dU are detected as C→T mutations when replication occurs in the cell. AID scans ssDNA processively thus ensuring that clones with mutations in *lacZ* are highly likely to contain mutations in IgV (20,22). Incubation conditions were chosen to ensure that ∼5% or fewer plaques were mutant (>95% dark blue wild type plaques) so that AID-generated dC deaminations were catalyzed principally by a single AID molecule scanning within the gapped DNA substrate (12,41).

The mutation spectrum of AID and Polη was compiled from 150 mutant phage clones containing 862 mutations (Figure 1). AID and Polη generated base substitutions throughout IgV, mainly in WRC motifs by AID (red), and WA motifs by Polη (yellow). There are three CDR regions each with a majority of C→T mutations located WRC/WRCW motifs: 75% in CDR1, 88% in CDR2, and 65% in CDR3 (Supplementary Table S3). A preferred mutagenic site in an overlapping AGCT motif near the 5′-end of CDR2 (position 144) also occurs *in vivo* in memory B- and Ramos B-cells (22). In contrast, the framework (FW) regions contain a minority of hot motif mutations: 40% in FW1, 0% in FW2, 32% in FW3, and 33% in FW4 (Supplementary Table S3). These observations reaffirmed the findings that CDR regions, which contain large numbers of WRC and WGCW hot motifs, are strategically favored sites of AID deamination compared to the FW regions (21,22,43), and that this characteristic is retained in the reconstituted biochemical system. Since CDR regions form the Ag binding site of an Ab, it is expected to be susceptible to more mutations than FW regions that encode the overall structure of the Ab and tend to be more conserved (44). The retention of AID and Polη signature activities when acting on *IGHV3-23*01 in vitro* suggested that perhaps they can be used to perform mutagenesis of Ab genes in a purified biochemical system that mimic *in vivo* IgV diversification in B-cells.

Diversification of a scFv 'mini synthetic' phage display library by AID and Polη

Data from the previous section showed that the combined action of AID and Polη on *IGHV3-23*01* demonstrated their suitability for V gene library diversification in our defined biochemical system. As a proof of principle for the application of AID and Polη to diversify an existing phage display scFv library, we have constructed a 'mini' synthetic scFv library using 18 heavy chain (V$_H$) and 20 light chain (V$_L$) chains. Combining V$_H$ and V$_L$ randomly provided 360 possible V$_H$–V$_L$ combinations, which constituted a mini
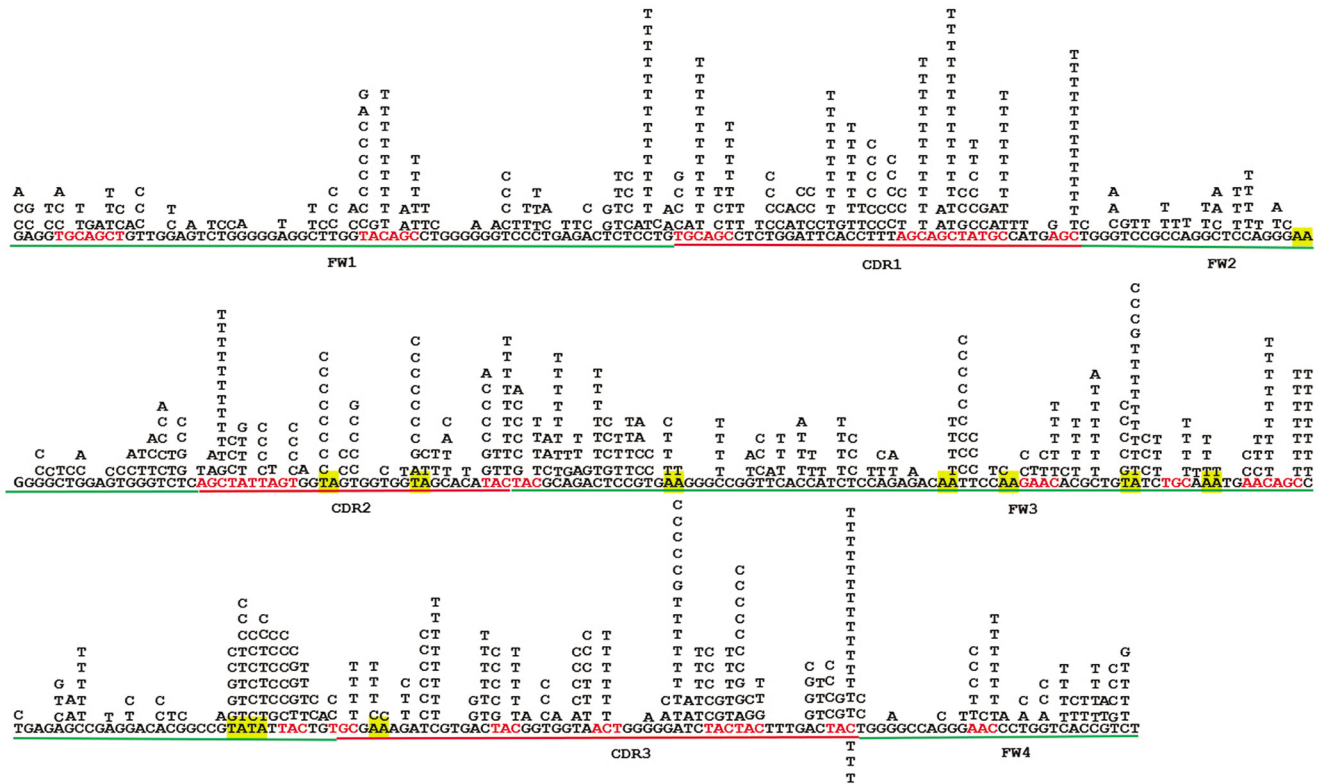
Figure 1. AID and Polη-catalyzed mutation spectrum on *IGHV3-23*01* region. A total of 862 AID and Polη-catalyzed mutations across the *IGHV3-23*01* gapped region in M13mp2 phage DNA construct were obtained from 150 mutated phage clones. Bases above the template sequence denote transition and transversion mutations occurring in mutant M13mp2 phage DNA. CDR1, CDR2 and CDR3 regions are indicated with red underlines and frameworks FW1, FW2, FW3 and FW4 regions - with green underlines. AID hot motifs (WRC/WGCW) and Polη (WA) hot motifs are in red font and highlighted in yellow, respectively. C→T mutation clusters are observed in WRC hotspots motifs (red) within CDR1 and CDR2 regions. T→C transition mutations, presumably done by Pol η, accumulate on TA (WA) hotspot motifs (yellow highlight).

scFv library that was then cloned into pADL-20c phagemid vector (see Materials & Methods).
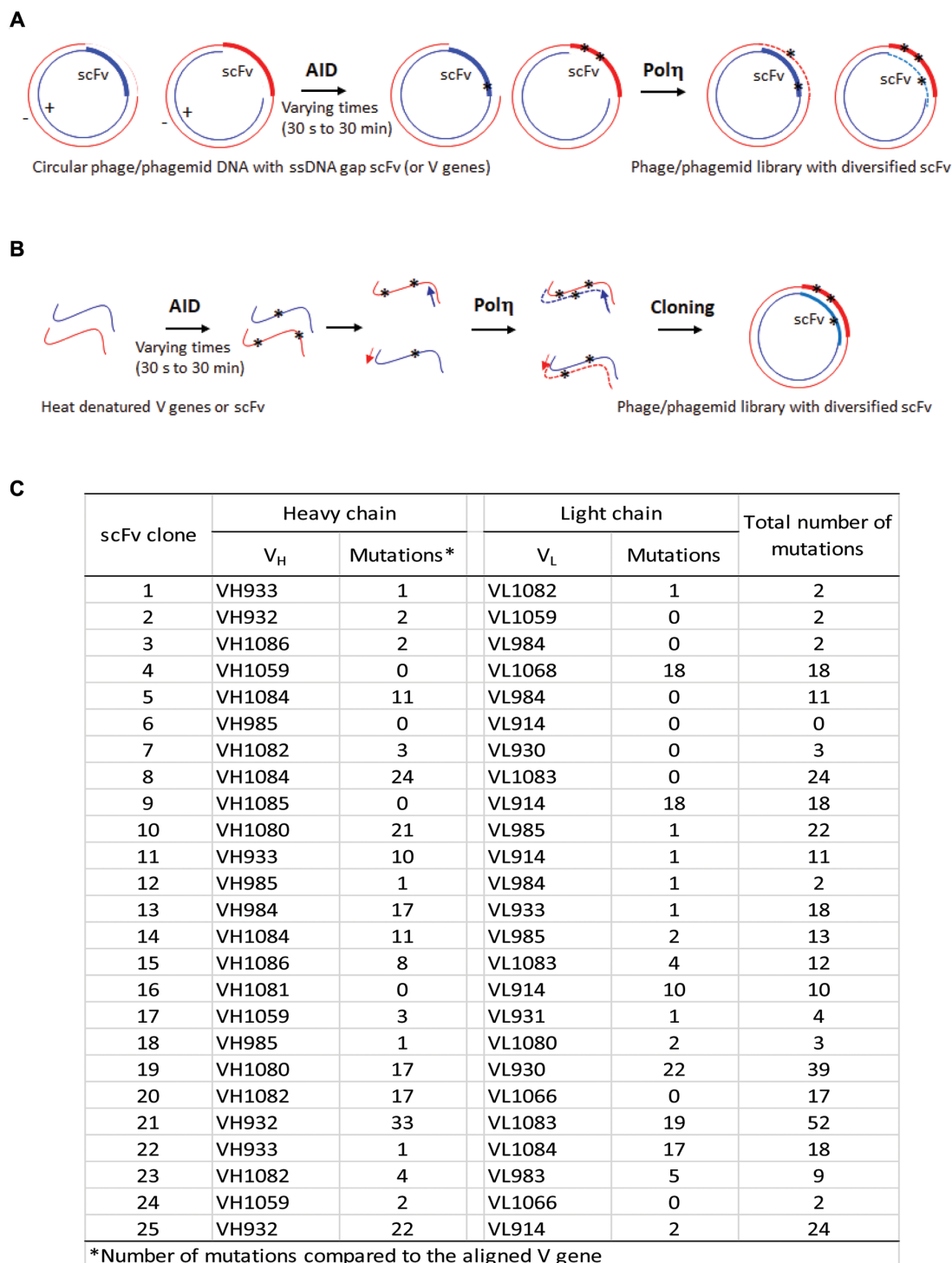
We constructed a 'double-gapped' dsDNA, containing an scFv within each ssDNA gapped region, for use as a substrate for AID and Polη to introduce mutations on both strands of scFv sequences (Figure 2A). To obtain a broad range of mutations in individual scFv clones, incubation of gapped substrates (500 ng) with AID (100 ng) was carried out for different incubation times (30 s, 45 s, 1 min, 2 min, 5 min, 10 min, 20 min and 30 min), followed by a gap filling synthesis with Polη (Figure 2A). The ensemble of mutagenized DNA molecules was used to transform *E. coli* (NR9404 *ung-*). The scFv library contained ∼5.4 × 10⁵ mutagenized clones. We compared the DNA sequences obtained from twenty-five arbitrarily chosen scFv clones with the original V_H and V_L sequence. The scFv clones contained a broad distribution of mutations, in a range between 0 and 52, with 0–33 in V_H and 0–22 in V_L (Figure 2C). There were individual clones containing multiple C→T and G→A mutations, along with mutations occurring at A and T sites, thereby showing that AID and Polη were able to act on both sense and anti-sense strands in the double-gapped substrate construct. For the purposes of illustration, a representative scFv clone (clone #25) was chosen to compare with the untreated heavy (VH 932) and light chains (VL914) (Supplementary Figure S1). AID-catalyzed processive deaminations were observed on both scFv strands as indicated

by the proximal locations of one C→T and nine G→A transition mutations on VH932, along with sixteen Polη-catalyzed mutations located both near and distal from the deamination sites (Supplementary Figure S1). The favored target specificities have been retained with elevated mutation frequencies observed in WRC and WA motifs for AID and Polη, respectively, favored in CDR in preference to FW regions. These data suggest that AID and Polη acting *in vitro* on scFv heavy and light chains may provide a sufficiently broad mutational landscape to facilitate diversification of scFv antibodies that could be used for selecting tight binders against a wide variety of antigens. A potential major advantage of this technique over standard phage display methods is that the scFv's selected initially can then be subjected to additional rounds affinity maturation *in vitro*.

Construction of AID- and Polη-diversified human scFv and Llama VHH phage display libraries

The key for a successful isolation of antibodies for specific antigens is the antibody gene library used for the selection. The ability to diversify variable regions (IgV) in a test tube provides a natural way (i.e. by analogy to IgV diversification in B-cells) to increase the size and complexity of existing or 'to-be-generated' human Ab repertoire libraries. Such Ab libraries would provide a powerful general toolkit for research, diagnostic and therapeutic purposes. We have

A

Circular phage/phagemid DNA with ssDNA gap scFv (or V genes) → Phage/phagemid library with diversified scFv

B

Heat denatured V genes or scFv → Phage/phagemid library with diversified scFv

C

scFv clone	Heavy chain		Light chain		Total number of mutations
	V_H	Mutations*	V_L	Mutations	
1	VH933	1	VL1082	1	2
2	VH932	2	VL1059	0	2
3	VH1086	2	VL984	0	2
4	VH1059	0	VL1068	18	18
5	VH1084	11	VL984	0	11
6	VH985	0	VL914	0	0
7	VH1082	3	VL930	0	3
8	VH1084	24	VL1083	0	24
9	VH1085	0	VL914	18	18
10	VH1080	21	VL985	1	22
11	VH933	10	VL914	1	11
12	VH985	1	VL984	1	2
13	VH984	17	VL933	1	18
14	VH1084	11	VL985	2	13
15	VH1086	8	VL1083	4	12
16	VH1081	0	VL914	10	10
17	VH1059	3	VL931	1	4
18	VH985	1	VL1080	2	3
19	VH1080	17	VL930	22	39
20	VH1082	17	VL1066	0	17
21	VH932	33	VL1083	19	52
22	VH933	1	VL1084	17	18
23	VH1082	4	VL983	5	9
24	VH1059	2	VL1066	0	2
25	VH932	22	VL914	2	24

*Number of mutations compared to the aligned V gene

Figure 2. Experimental strategies for *in vitro* diversification of IgV or scFv using AID and Polη. (**A**) Schematic diagram illustrating *in vitro* mutagenesis of phage/phagemid gapped substrates by AID and Polη. Circular phage/phagemid DNA containing ssDNA regions of scFv (or IgV) on plus (+), or minus (–) strands were subjected to deamination by incubation with AID for incubation times from 30 s to 30 min at 37°C. Pooling of AID-treated reactions for the different reaction times resulted in DNA clones containing a wide range of mutations at G/C sites. Mutations were introduced at A/T sites by subsequent incubation of the AID-treated scFv DNA with Polη. Following AID and Polη treatment, the DNA molecules were pooled and used to transform *E. coli* to make a diversified scFv phage/phagemid library. (**B**) Diversification of V genes or scFv fragments by AID and Polη. V genes or scFv fragments were denatured at 95 °C for 2 min, then rapidly cooled and treated with AID at 37°C for incubation times from 30 s to 30 min, to introduce mutations at G/C sites. The DNA pool of AID-treated V genes (or scFv fragments) was annealed to primers and subjected error-prone synthesis by Polη to introduce mutations at A/T sites. Subsequently, diversified scFv libraries were obtained by PCR amplification and cloning of AID- and Polη-treated V genes (or scFv fragments) into a phage/phagemid vector. (**C**) Distribution of mutations in 25 randomly sequenced representative scFv clones from AID- and Polη-diversified synthetic scFv library. Heavy (V_H) and light (V_L) chain identities and numbers of mutations caused by AID and polη are shown for each sequenced scFv clone.

incorporated AID and Polη-mediated V gene diversification steps during construction of human Ab gene libraries to make a sizable scFv phage display library containing $\sim 1 \times 10^9$ independent scFv phage clones.

A strategy to construct human diversified scFv libraries by AID and Polη

We constructed an AID- and Polη-diversified human scFv library and cloned in a type 3 trypsin release f3TR1 phage display vector (31). The library was constructed in following steps (see Materials and Methods): (i) heavy chain V_H and light chain V_L (V_κ and V_λ) gene repertoires were PCR amplified from tonsil naïve B-cell cDNA using a set of subfamily-specific forward and reverse primers. In a second PCR step, adaptor sequences were incorporated onto the ends of heavy and light chains, thereby allowing the random fusion of heavy and light chains via a flexible $(G_4S)_4$ linker by overlapping PCR, carried out in a later step. BglI restriction sites are added at the 5′-end of V_H and 3′-end of V_K and V_L for subsequent cloning into a phage vector; (ii) V gene repertoires were denatured by heating at 95°C for 2 min, rapidly chilled and incubated with AID at 37°C to allow dC deaminations on both denatured ssDNA strands resulting in C to T or G to A mutations (Figure 2B). Since longer incubation times lead to higher average numbers of AID-induced mutations on ssDNA substrates, individual reactions were carried out using a wide range of incubation times (30 s, 45 s, 1 min, 2 min, 5 min, 10 min and 20 min) and were then combined to broaden the range of mutations on individual scFv molecules; (iii) AID-treated V genes were annealed to primers and one round of Polη extension synthesis was carried out to introduce mutations at A and T sites (Figure 2B); (iv) Overlapping PCR was used to generate an scFv gene repertoire. The scFv PCR products were digested with BglI and directionally ligated into BglI sites of a f3TR1 phage vector. Ligated DNA molecules were transformed into MC1061 *E. coli* cells by electroporation. A total of 240 independent electroporations were carried out to generate a human f3TR1-scFv library containing 1.1×10^9 independent phage clones.

The diversity of the scFv repertoire and the quality of the primary library were examined by PCR analysis and by sequencing DNA segments encoding the scFv genes from 16 randomly picked f3TR1-scFv clones. Based on an analysis of 16 clones by PCR, using primers flanking the BglI sites, we determined that 15 clones (94%) contained an insert corresponding to the correct scFv size. Sequencing performed on 16 scFv clones showed that each of the clones contained different combinations of heavy V_H and light V_L (V_κ and V_λ) chains (Supplementary Table S4). The variable regions were derived from 12 different V gene families, composed of five V_H gene families (V_{H1}, V_{H2}, V_{H3}, V_{H4} and V_{H6}) and seven V_L gene families consisting of both kappa and lambda light chains ($V_{\kappa1}$, $V_{\kappa2}$, $V_{\kappa3}$, $V_{\kappa5}$ and $V_{\lambda1}$, $V_{\lambda3}$, $V_{\lambda6}$). The CDR3 of V_H sequences were diverse, with lengths between 9 and 19 amino acids. The CDR3 of V_L chains contained 9–12 amino acids (Supplementary Table S4).

Thus, the scFv regions were distributed across a wide repertoire of antibody germ line genes. The range of mutations were 0–32 for V_H and 0–48 for V_L. Two V genes had no mutations indicating the absence of affinity maturation in B-cells and in our biochemical system (Supplementary Table S4). In contrast, the presence of multiple mutations within a large majority of V_H and V_L genes demonstrates the occurrence of affinity maturation taking place either during a secondary immune response in B-cells *in vivo* or during exposure to AID and Polη *in vitro*. Nevertheless, using, for example, a representative scFv clone (F3), we can identify *in vitro* AID signature C→T and G→A mutations unambiguously by comparison with the germ line sequence (Supplementary Figure S2). Compared to the germ line, V_H contains four C→T mutations, and V_L contains nineteen C→T or G→A mutations. There are also other mutations that were probably generated by error-prone replication by Polη. The *in vitro* contributions by AID and Polη are also shown by the presence of mutations occurring in the linker sequences that were added to the second PCR primers used to fuse V_H and V_L in to generate the scFv library. Among sixteen clones, nine have no linker mutations, while five contain C→T or G→A mutations and two contain mutations at non-C/G sites (Supplementary Figure S3).

Diversification of Llama's VHH naïve library by AID and Polη

Llamas produce functional Abs that lack light chains. The variable domain of llama heavy chain Ab molecules (VHH) contains three CDR regions that are fully capable of antigen recognition (30,45). A naïve Llama VHH phage library (Abcore, Ramona, CA) was used to generate an AID-Polη mutagenized f3TR1-VHH library. Amplification from the naïve library was carried out with forward and reverse primers that contained BglI restriction sites, which allowed the subcloning of VHH into an f3TR1 phage vector. Mutagenesis of VHH by AID and Polη were performed as for the human scFv. The diversified VHH constructs were transformed into *E. coli* MC1061 using 160 electroporations to obtain a mutagenized f3TR1-VHH phage library containing $\sim 2.8 \times 10^8$ independent clones.

Application of AID and Polη-mediated affinity maturation in a purified biochemical system to isolate antibodies targeting specific antigens

Since affinity maturation of B-cells involves multiple rounds of SHM in IgV regions after antigen exposure, followed by the clonal selection of target-specific Abs, we sought to simulate this *in vivo* process by focusing on single Ab clones selected against a specific target. From the human scFv and llama-VHH phage-displayed libraries, a subset of antibody candidates displaying target-specific affinity toward selected antigens was isolated via conventional biopanning. We chose three antigen targets: (i) human glucagon-like peptide-1 receptor (GLP-1R); (ii) human fatty acid amide hydrolase (FAAH); (iii) mouse artemin neurotrophic factor. The isolated Ab clones were subjected to further *in vitro* affinity maturation using AID and Polη, followed by additional rounds of biopanning of the 'affinity-matured' sublibrary (GLP-1R) or single Ab clones (FAAH). Peptides of the original and affinity-matured Ab clones were purified, and their sequences and binding affinities examined to eval-

uate the effects of *in vitro* affinity maturation for individual clones.

Isolation of eight GLP-1R specific human scFvs from an AID and Polη-diversified human-scFv library and subjected to in vitro affinity maturation

Glucagon-like peptide-1 receptor (GLP-1R) is a Family B G-Protein Coupled Receptor (GPCR) for glucagon-like peptide 1(GLP-1) hormone, which stimulates glucose-induced insulin secretion (46,47). Based on its central role in glucose metabolism, GLP-1R is a major therapeutic target for the treatment of type II diabetes.

The human mutagenized scFv-phage library was used in four rounds of biopanning against GLP-1R-expressing *Sf9* cells. Phage titration and amplification were done as described (Materials and Methods). Two additional rounds of biopanning were performed on the combined third and fourth panning output phages using purified GLP-1R protein immobilized on a polystyrene immunotube. Ninety-six individual clones from the final sixth panning output were randomly picked for screening by phage-ELISA, and positive binders were identified as those with signals ≥3-fold above background (Figure 3A). Eight scFv clones were isolated and sequenced. The binding affinity of each scFv peptide to GLP-1R was measured by plotting the binding ELISA signal (A_{450} nm) versus the concentration of purified scFv peptide (Figure 3B–D).

To accommodate the iterative nature of B-cell affinity maturation into our Ab optimization strategy, eight GLP-1R-specific scFv clones to were subjected to further AID and Polη *in vitro* affinity maturation. After AID and Polη treatment of the scFv, the mutagenized clones were transformed into *E. coli* to obtain a sub-library of mutagenized scFv-phage. Ninety-six individual clones from the 3rd round of biopanning were randomly picked for screening. An scFv clone (GHM33) displaying high affinity originated from GHM 25, which is one of the eight original scFv clones. GHM33 contains T220M and S243C amino acid replacements (Supplementary Figure S4B), that correspond to an AID-induced C→T mutation in V_L- FW3, and a Polη-induced C→G mutation in V_L- CDR3 (Supplementary Figure S4). The affinity measurements for GHM 25-scFv and its affinity-matured variant, GHM 33-scFv were determined using phage-ELISA (Figure 4A) and peptide-ELISA (Figure 4B). The affinity matured GHM33-scFv phage clone bound to GLP1R with about a two-fold higher affinity (A_{450} nm ∼ 0.6) compared with GHM25-scFv (A_{450} nm ∼ 0.3) (Figure 4A). Based on ELISA, the purified GHM33 peptide had an apparent EC_{50} ∼95 nM, which was about 3-fold lower than that of the parental scFv (302 nM). Therefore, there appeared to be an approximate 3-fold increase in the binding affinity following a single round of affinity maturation *in vitro*.

Application of affinity maturations steps *in vitro* on single clones to isolate FAAH specific llama-VHH nanobodies

FAAH is an integral membrane enzyme responsible for the hydrolysis of anandamide and 2-arachidonoylglcerol in the endocannabinoid system, which has been involved in chronic pain treatment for decades (48,49). Genetic or pharmacological inactivation of FAAH has shown analgesic, anti-inflammatory, anxiolytic and antidepressant response while apparently causing no undesirable side effects (50). Although FAAH inhibitors have been studied for years, nonspecific binding of the inhibitors hindered these studies and drug development.

The llama naïve and mutagenized f3TR1-VHH library was subjected to three rounds of panning against purified human FAAH protein. One VHH (clone A3) with high affinity toward FAAH was isolated from the naive VHH-phage library. Subsequently, AID-Polη *in vitro* affinity maturation was performed on A3 to improve its FAAH binding affinity. The affinity maturated VHH-phage library was subjected to three rounds of biopanning with increasingly higher blocking buffer concentrations, lower amount of immobilized antigen, and more stringent washing steps. From the screening of 96 individual clones from the last panning output, 20 clones with the highest binding signals for FAAH were picked for sequence analysis. Two clones with unique amino acid sequences (Supplementary Figure S5A) were isolated and purified along with the original A3-VHH. Their equilibrium dissociation constants (K_D) were measured by surface plasmons resonance (Table 1).

Two affinity-matured VHH clones, F9 and OD1, showed increased affinity toward FAAH compared to the parental clone, A3 (K_D ∼ 1.56 nM). F9 (K_D ∼ 1.26 nM) showed slightly increased affinity with a T→C and a A→T mutations in the FW1 and FW2 regions (Supplementary Figure S5A). Yet, only one amino acid change was found in the FW1 region (Supplementary Figure S5B). OD1 (K_D ∼ 0.65 nM) showed about 2.4-fold enhanced affinity to FAAH than the parental VHH. A total of four different mutations were found throughout FW1, CDR1, CDR2 and FW3, respectively, in OD1 compared to the parental sequence A3, attributed to a single amino acid change, Y81F, in the FW3 region (Table 1).

Isolation of Artemin-specific llama-VHH from naïve and affinity matured libraries

Artemin is a glial cell-line derived neurotrophic factor that serves as a ligand for the neurotrophin receptor GFRα3 that has been shown to be required for increased sensitivity to cold after either an inflammatory or neuropathic injury (36,37). Our prior work has shown that monoclonal antibodies raised against artemin can lead to a transient inhibition of cold allodynia (cold pain to an otherwise innocuous cold stimulus) in mice (37). Therefore, the development of monoclonal antibodies targeting artemin could provide an effective therapeutic treatment to alleviate cold hypersensitivity. To address the effects of *in vitro* affinity maturation on an Ab repertoire prior to antigen exposure, we performed a parallel selection on a naïve VHH library and on an AID-Polη mutagenized VHH library. After three rounds of panning against artemin, two nanobodies in mutagenized and naïve libraries were identified. Two clones LM41 and LM52 from the VHH mutagenized library represent AID-Polη induced mutant variants of LU68 and LU5 clones from the naïve VHH library. LM52 from the mutagenized library had identical DNA sequences to LU5 except
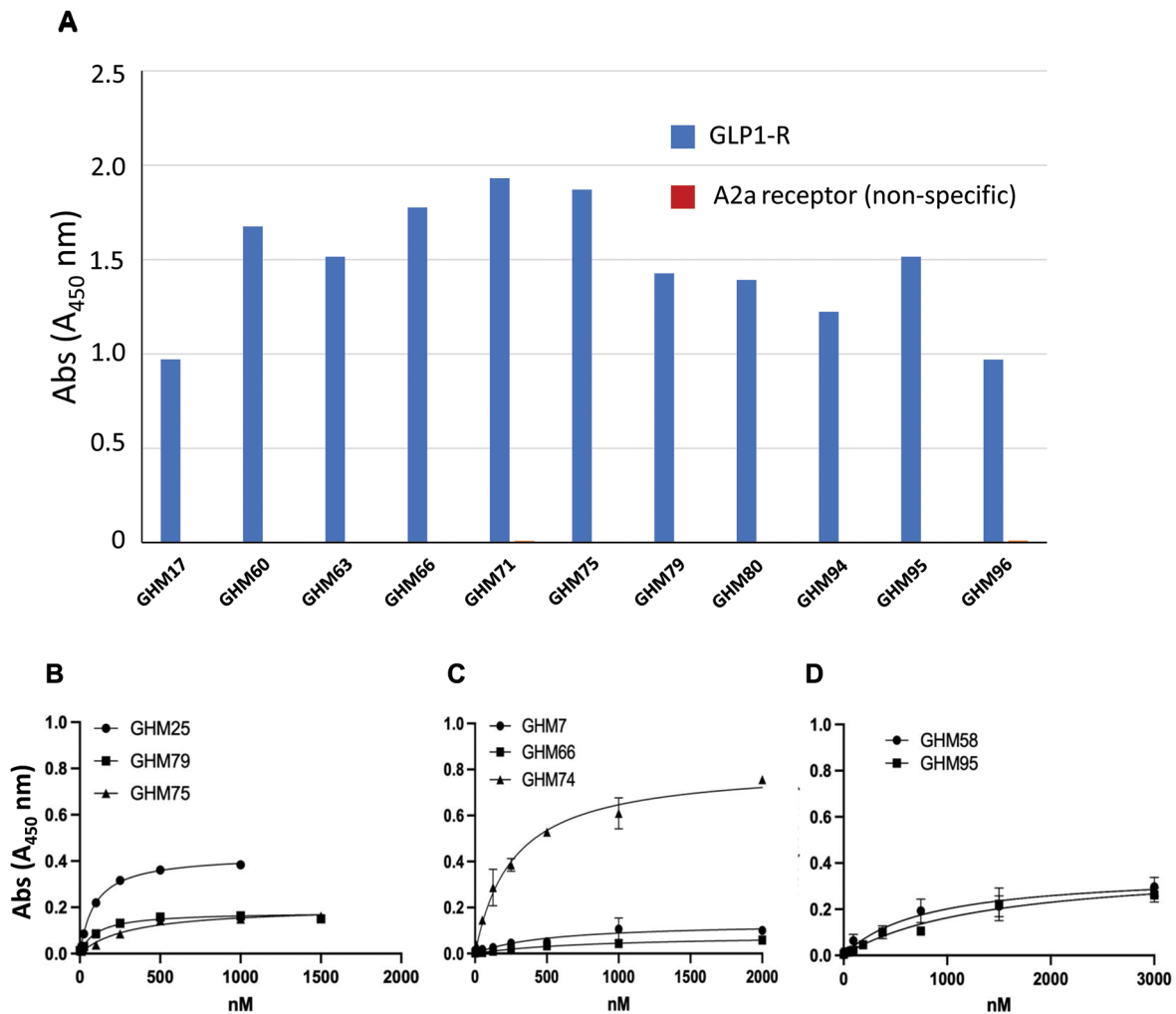
Figure 3. ELISA screening of GLP-1R specific *scFv*s isolated from AID and Polη-diversified human scFv library. (**A**) Specific binding of 11 individual scFv-phage to purified human GLP1-R. Phage ELISA was carried out by immobilization of 1 μg of recombinant GLP1-R and a negative control protein, adenosine A2a receptor protein (A2a), in wells of a Nunc 96-well Maxisorp plate and incubated with 10^8 transducing unit (TU) of scFv-phage. Binding of scFv phage was detected by immunodetection of the phage coat protein p8 by anti-M13 p8 conjugated with HRP. ELISA absorbance A_{450} nm values for A2a control are represented as red bars, whereas the A_{450} nm values for GLP1-R are represented as blue bars. (**B–D**) ELISA binding assay for eight purified anti-GLP-1R scFv: (**B**) GHM25, GHM75 and GHM79, (**C**) GHM7, GHM66 and GHM74, and (**D**) GHM58 and GHM95. The absorbance (A_{450} nm) values for A2a at each concentration of scFvs were used as non-specific binding ELISA backgrounds. The absorbance (A_{450} nm) values for GLP1-R after substracting the background are shown as averages ± standard deviations in the binding curves. Assays for all scFvs were performed at the same time. Binding curves are presented in separate panels for presentation purpose.

that it contained two G→A, one C→T mutations, indicative of AID deaminations, and T→C and T→A mutations, that was most likely generated by Polη (Supplementary Figures S6A,). The dC deaminations were found to be 5∼7 bases apart, thereby reflecting the processive action of AID (12,51). The resulting changes in amino acid composition in LM52 were Y62H, A78T, T80M and N89K (Table 2, Supplementary Figure S6C), which were contained in the FW3. A second pair, LU68 and LM41, share identical sequences except at ∼150 bp downstream of the start codon, where two T→C substitutions have been added 9 bases apart from each other in WA (W = A/T) sites, which correspond to the Polη hot motif (Supplementary Figure S6B). One mutation was observed in CDR2, with a second in FW3. There was a single amino acid change in LM41 (Y62H) located in the FW3 (Table 2, Supplementary Figure S6D).

VHH peptides isolated from naïve and mutagenized libraries were purified, and binding to artemin was measured by surface plasmons resonance. The mutated VHH-artemin binding affinities were increased compared to their parental counterparts (Table 2). Affinity matured LM41 bound about 4-fold more strongly ($K_D \sim 111$ nM) than its nonmutated parent LU68 ($K_D \sim 456$ nM). Another mutated nanobody, LM52, showed a more modest ∼1.7-fold increase in binding ($K_D \sim 102$ nM) compared to LU5 ($K_D \sim 178$ nM) (Table 2).

We tested one of the affinity matured VHH fragments (LM52) to determine its ability to inhibit artemin-mediated cold pain *in vivo*, i.e. to specifically inhibit artemin-mediated cold hypersensitivity that occurs with injury. Mice behavioral assays were performed using one of the four VHH peptides, LM52, along with a positive control
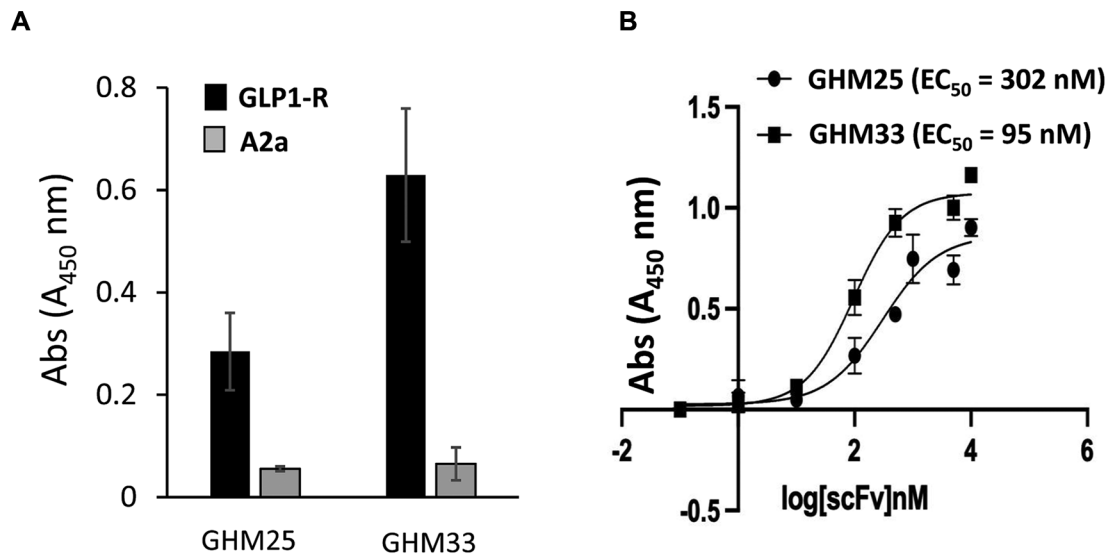
Figure 4. GLP1-R binding of anti-GLP1-R scFv clone (GHM 25) and its AID- and Polη-affinity matured clone (GHM33). (**A**) Phage-ELISA based binding of GHM25 and GHM33 human-scFv to purified GLP1-R whole membrane protein. Human GLP1-R and A2a background binding control was immobilized on each well of a Nunc 96-well Maxisorp plate and incubated with GHM33-scFv or GHM25-scFv phage. Binding of scFv-phage was measured by immunodetection of the phage coat protein pIII by anti-M13 pIII mAb conjugated with HRP. Error bars represent the standard deviations of four trials. (**B**) Concentration-dependent binding of purified GHM25 and affinity-matured GHM33 scFv peptides to GLP1-R measured by ELISA. GLP1-R was immobilized on Nunc maxisorp plate and incubated with increasing concentration (1 nM, 10 nM, 100 nM, 500 nM, 1 μM, 5 μM, 10 μM) of each c-myc tagged scFvs, GHM25 (circle) and GHM33 (square). Binding of scFv was followed by immunodetection of the C-myc tag using anti-c-myc antibody conjugated with HRP. Error bars represent the standard deviation of duplicates. Apparent EC_{50} was estimated from the Abs (A_{450} nm) vs. log[scFv] graph.

Table 1. Kinetic and equilibrium dissociation constants of purified llama-VHH nanobodies targeting fatty acid amide hydrolase (FAAH)

Clone*	k_{on} ($M^{-1} S^{-1}$)E^{+4}	k_{off} (S^{-1})E^{-4}	K_D (nM)	Amino acid change
A3 (original)	3.64	0.57	1.56	
F9 (affinity matured)	16.9	2.14	1.26	V14A
OD1 (affinity matured)	16.5	1.07	0.65	Y81F

*Clones F9 and OD1 represent affinity matured variants of clone A3, which were obtained after one round of *in vitro* affinity maturation by AID and Polη.

Table 2. Kinetic and equilibrium dissociation constants of purified llama-VHH nanobodies targeting artemin

| Clone*	k_{on} ($M^{-1} S^{-1}$)E^{+5}	k_{off} (S^{-1})E^{-2}	K_D (nM)	Amino acid change
LU68 (naive)	0.50	2.30	456	
LM41 (mutated)	0.46	0.52	111	Y62H
LU5 (naive)	0.49	0.88	178	
LM52 (mutated)	0.39	0.40	102	A78T, T80M, N89K

*Clones LU68 and LU5 were isolated from a Llama-VHH naïve library and clones LM41 and LM52 were from an AID- and Polη-diversified library.

(a full-length anti-mouse artemin monoclonal antibody, MAB1085 (R&D Systems) which we have shown specifically alleviates cold allodynia (37) (Figure 5). To induce cold pain, wildtype mice were given a single intraplantar injection of CFA and then tested two days later when cold allodynia was observed in the injected (ipsi) hind paw compared to the un-injected hind paw (contra) (Figure 5). Mice were then given a subcutaneous nape injection of either

MAB1085 or LM52 nanobody (10 mg/kg body weight) (Arrows, Figure 5A and B) and then we measured cold sensitivity over the next several hours. In both groups of mice injected with LM52 or MAB1085, an increase in withdrawal latencies was observed over time above the post-CFA level 1–4 h post-injection, indicating attenuation of cold allodynia and reduced pain (Figure 5). Although LM52 nanobody took longer (4 h post-injection) to fully restore the cold response back to the pre-CFA level (Figure 5B) compared to the positive control (1 h post-injection) (Figure 5A), its inhibitory effect on artemin-mediated cold pain was evident from the increasing trend in the withdrawal latency post-nanobody injection. For LM52, the inhibitory effect appeared to be waning by 12 hours (MAB1085 injected mice were not tested beyond the 4 h time point), likely indicating a loss of binding between the nanobody and artemin. In 24 h, cold allodynia was fully recovered in both MAB1085 and LM52 nanobody injected mice. The mice studies revealed that LM52 nanobody is not only specific to artemin, but also inhibits artemin function to suppress cold allodynia *in vivo*.

DISCUSSION

This is the first study, to our knowledge, that uses AID and Polη in a biochemical system to target mutations to DNA sequence motifs in IgV that favor the generation of Ab-Ag high-affinity binders. Here we show that AID and polη can recapitulate the key enzymatic and motif preferences known from their function in the vertebrate immune system. From this finding, we developed a method for the biochemical reconstitution of B-cell affinity maturation using these puri-
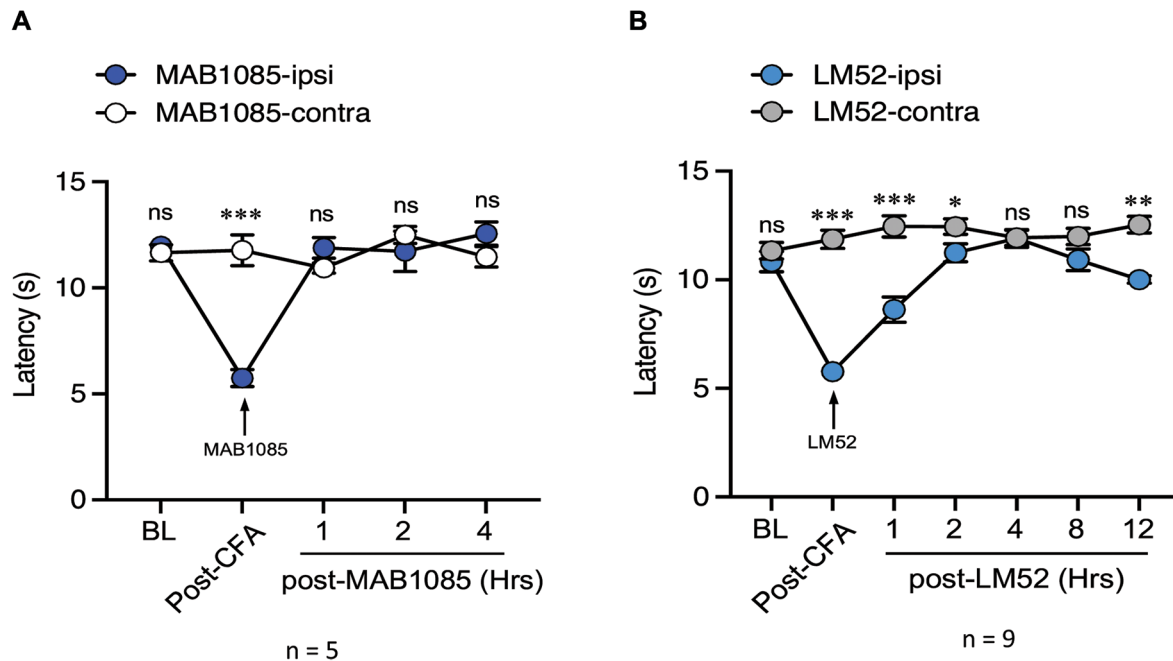
Figure 5. Inflammatory cold allodynia is reduced in mice treated with anti-artemin full length IgG and VHH nanobody. CFA induced hind paw cold allodynia in mice, indicated by a decrease in cold-evoked hind paw withdrawal latencies 2 days post-injection, was significantly attenuated when mice were treated with either anti-artemin (**A**, $n = 5$) MAB1085 (R&D systems) or (**B**, $n = 9$) LM52-VHH. The extent of cold sensitization was determined by comparing the pre- to post-CFA injection latencies. Each animal was then given an s.c. injection of 10 mg/kg body weight of each Ab and changes in cold sensitivity were compared in the CFA-injected, ipsilateral (ipsi) hind paw to the control, un-injected contralateral paw (contra). ns, $P > 0.05$, *** $P < 0.001$, ** $P < 0.01$, * $P < 0.05$.

fied SHM enzymes and phage display. We first examined the combined AID and Polη mutation profiles on human *IGHV3-23*01* and a scFv gene repertoire to assess whether the application of AID and Polη in biochemically reconstituted systems captures the salient features of B-cell SHM. Earlier studies showed that during SHM, AID and Polη: (i) introduce mutations on IgV at a high rate, approximately million-fold higher than the basal level of mutation elsewhere in the genome (16,17); (ii) introduce mutations preferentially on WRC and WA hotspot motifs (52,53), particularly in the CDR regions (21,22,43) and (iii) retain their catalytic specificities in both B cells and in cell-free systems, as evidenced by their similar mutation profiles *in vivo* and *in vitro*. The mutation profile in *IGHV3-23*01* generated by the AID and Polη exhibited these signature characteristics, demonstrated by the broad spectrum of substitutions covering the entire IgV region, accumulation of AID-induced deaminations in WRC hotspot motifs, and Polη-induced substitutions in WA motifs, particularly in the CDR regions (Supplementary Table S1).

Currently, there are three principal sources of therapeutic monoclonal Abs. These include Abs produced in transgenic mice, humanized Abs, and Abs selected using *in vitro* phage and yeast display (54–56). These technologies have made significant inroads toward generating extensive repertoire of human mAbs, owing largely to advances in 'antibody engineering', library construction, and high throughput screening that allows for the selection for Ab binding to favored Ag targets along with counter selection against disfavored Ab–Ag binding. However, achieving useful therapeutic Abs typically require additional steps, often involv-

ing the use of *in vitro* affinity maturation methods to optimize targeting affinities and specificities (57,58). Methods that have been developed for *in vitro* Ab affinity maturation include random mutagenesis (59), targeted mutagenesis (60), and saturated mutagenesis using a synthetic combinatorial Ab library (61). Random mutagenesis of V-genes is usually carried out by PCR with a low fidelity DNA polymerase (59). However, random mutations are unlikely to have mutation profiles characteristic of V-gene SHM, and also have limited ability to generate multiple mutations in individual Ab clones. Multiple mutations are often necessary to significantly improve Ab-Ag binding affinities (61,62). Targeted mutagenesis involves site-directed mutagenesis in Ig CDR sequences (60), which while a potentially effective strategy, is nevertheless based on an arbitrary *a priori* choice for which motifs to mutate. The combinatorial methods, although potent, are labor intensive, requiring massive synthesis of DNA oligonucleotides at each selection round along with a need for expansive libraries to produce sufficiently large numbers of Ab variants (63).

Since the production of sizable numbers of antibody variants is essential to achieve selective high-affinity Ab–Ag binding using *in vitro* affinity maturation, a quick and efficient technique to diversify and, if necessary, re-diversify V gene sequences is the subject of this paper. We suggest that a strategy for *in vitro* affinity maturation using AID and Polη, by partial analogy to B-cell affinity maturation, provides a relatively simple, labor 'light' and efficient new method to diversify V gene sequences and Ab libraries. Since IgV gene sequences have evolved in B-cells via mutagenesis by AID and Polη, the application of AID and Polη to diversify V

genes in a test tube seems likely to result in a smaller number of non-productive V gene variants. In contrast to random and targeted mutagenesis, AID and Polη can produce broad clonal heterogeneity in scFv molecules, which contain large variations in the numbers and locations of mutations. We have found that mutation numbers range from 0 to 33 in V_H and 0–22 in V_L among 25 randomly picked individual clones (Figure 2C). Furthermore, since AID and Polη are able to generate V gene mutations that mimic natural SHM mutations in activated B-cells, the Abs seem likely to be tolerated by the human immune system. Most notably, the capability to mutagenize IgV using AID and Polη, select for Ab–Ag binders, and then perform subsequent mutagenesis and selection steps, distinguishes our methodology from these other methods to generate mAbs *in vitro*. This is not a 'one and done' process. Rather, our reiterative Ab maturation method has the clear potential to obtain Abs with higher and higher Ag binding affinities and selectivity, at each mutagenesis and selection step.

An analysis of AID- and Polη-induced mutations obtained from a sample of 20 randomly selected scFv clones reinforced the observation that mutation frequencies were favored in CDR over FW regions (Supplementary Table S2). We applied the biochemical mutagenesis strategy to introduce mutations into naive human-scFv and llama-VHH libraries. However, owing to the presence of *in vivo* AID and Polη-induced mutations in naïve V-gene repertoires, we cannot distinguish unambiguously between mutations introduced by AID and Polη in individual Ab clones *in vitro* versus *in vivo*. Nevertheless, sequence characterization of random scFv clones selected from the mutagenized human-scFv library showed that mutations have been successfully introduced during the library construction step, indicated by the substitution mutations in the consensus linker sequence of known sequence identity (Supplementary Figure S3). Furthermore, the observed broad mutational heterogeneity in mutated scFv from the mutagenized mini synthetic library (Figure 2C, Supplementary Figure S1) provides a 'proof-of-principle' for the application of AID and Polη to diversify any existing Ab library, and higher affinity Abs are obtained following subsequent mutagenesis and selection steps during the *in vitro* affinity maturation process.

The effectiveness of the strategy was evaluated by comparing Ab–Ag apparent binding affinities using scFv/VHH clones of known sequence identities before and after *in vitro* mutagenesis. We observed 3-fold tighter binding in an anti-GLP1-R scFv GHM33 picked from a sub-library containing eight mutagenized scFvs compared to the parental clone (GHM 25) (Figure 4). The seemingly beneficial mutations occurred at T220M and S243C. A second application involved one round of *in vitro* affinity maturation of single VHH clone specifically binding to FAAH. Each of the two variants originated from clone A3 showed improved affinity toward FAAH, with OD1 exhibiting ∼2.4-fold enhanced binding compared to the parental clone on SPR assay (Table 1). The AID and Polη diversified phage-VHH library originated from a single, A3, clone which binds tightly to FAAH, with a $K_D = 1.56$ nM. Thus, there might have been little room for improvement for this clone and the fact that the library diversification was carried out on only a single

genome sequence might have limited the diversity of mutations. Additionally, there was only one round of affinity maturation performed for this library. In the germinal center, multiple rounds of affinity maturation were done followed by the selection process to improve the antibody affinity. We would expect to see a higher fold of affinity increment from more selection and affinity maturation rounds.

A third application selected for tighter binding VHH nanobodies against artemin. One of the affinity matured clones, LM41, showed a 4-fold increased binding affinity ($K_D = 111$ nM, Y62H) compared to the parental clone, LU68 ($K_D = 456$ nM) (Table 2). A second affinity matured clone, LM52, which showed a more modest ∼1.7-fold increased binding affinity (Table 2), was nevertheless reasonably effective in its ability to inhibit artemin-mediated cold sensitivity in a mouse model (Figure 5). Not surprisingly, the VHH nanobody, was less effective in ameliorating the cold sensitivity symptoms than a fully mature antibody against artemin, with the mouse retaining deleterious cold sensitivity for about twice as long for the nanobody (Figure 5B, 2 h latency) compared to treatment with the full-length Ab (Figure 5A, 1 h latency). However, the data show that even a relatively weakly affinity matured VHH binder is nevertheless able to function surprisingly effectively *in vivo*, and represents a proof-of-principle, admittedly modest at present, but demonstrating sufficient potential for future development. Two short-term next steps are both straightforward and likely to result in an immediate improvement. The first is to carry out additional affinity maturation on a tightest binder or perhaps using a mix of tightest and more moderate binders. Second, perform the panning steps by varying elution buffer conditions to optimize Ab–Ag selection stringency.

SUPPLEMENTARY DATA

Supplementary Data are available at NAR Online.

ACKNOWLEDGEMENTS

FUNDING

REFERENCES

1. Bradbury,A.R., Sidhu,S., Dubel,S. and McCafferty,J. (2011) Beyond natural antibodies: the power of in vitro display technologies. *Nat. Biotechnol.*, **29**, 245–254.
2. Mattheakis,L.C., Bhatt,R.R. and Dower,W.J. (1994) An in vitro polysome display system for identifying ligands from very large peptide libraries. *Proc. Natl. Acad. Sci. U.S.A.*, **91**, 9022–9026.
3. Smith,G.P. (1985) Filamentous fusion phage: novel expression vectors that display cloned antigens on the virion surface. *Science*, **228**, 1315–1317.
4. Boder,E.T. and Wittrup,K.D. (1997) Yeast surface display for screening combinatorial polypeptide libraries. *Nat. Biotechnol.*, **15**, 553–557.
5. Ho,M. and Pastan,I. (2009) Mammalian cell display for antibody engineering. *Methods Mol. Biol.*, **525**, 337–352.
6. Schier,R., McCall,A., Adams,G.P., Marshall,K.W., Merritt,H., Yim,M., Crawford,R.S., Weiner,L.M., Marks,C. and Marks,J.D. (1996) Isolation of picomolar affinity anti-c-erbB-2 single-chain Fv by molecular evolution of the complementarity determining regions in the center of the antibody binding site. *J. Mol. Biol.*, **263**, 551–567.
7. Little,M., Breitling,F., Micheel,B. and Dubel,S. (1994) Surface display of antibodies. *Biotechnol. Adv.*, **12**, 539–555.
8. Wark,K.L. and Hudson,P.J. (2006) Latest technologies for the enhancement of antibody affinity. *Adv. Drug. Deliv. Rev.*, **58**, 657–670.
9. Di Noia,J.M. and Neuberger,M.S. (2007) Molecular mechanisms of antibody somatic hypermutation. *Annu. Rev. Biochem.*, **76**, 1–22.
10. Peled,J.U., Kuang,F.L., Iglesias-Ussel,M.D., Roa,S., Kalis,S.L., Goodman,M.F. and Scharff,M.D. (2008) The biochemistry of somatic hypermutation. *Annu. Rev. Immunol.*, **26**, 481–511.
11. Muramatsu,M., Kinoshita,K., Fagarasan,S., Yamada,S., Shinkai,Y. and Honjo,T. (2000) Class switch recombination and hypermutation require activation-induced cytidine deaminase (AID), a potential RNA editing enzyme. *Cell*, **102**, 553–563.
12. Pham,P., Bransteitter,R., Petruska,J. and Goodman,M.F. (2003) Processive AID-catalysed cytosine deamination on single-stranded DNA simulates somatic hypermutation. *Nature*, **424**, 103–107.
13. Bransteitter,R., Pham,P., Scharff,M.D. and Goodman,M.F. (2003) Activation-induced cytidine deaminase deaminates deoxycytidine on single-stranded DNA but requires the action of RNase. *Proc. Natl. Acad. Sci. U.S.A.*, **100**, 4102–4107.
14. Chaudhuri,J., Tian,M., Khuong,C., Chua,K., Pinaud,E. and Alt,F.W. (2003) Transcription-targeted DNA deamination by the AID antibody diversification enzyme. *Nature*, **422**, 726–730.
15. Sohail,A., Klapacz,J., Samaranayake,M., Ullah,A. and Bhagwat,A.S. (2003) Human activation-induced cytidine deaminase causes transcription-dependent, strand-biased C to U deaminations. *Nucleic Acids Res.*, **31**, 2990–2994.
16. McKean,D., Huppi,K., Bell,M., Staudt,L., Gerhard,W. and Weigert,M. (1984) Generation of antibody diversity in the immune response of BALB/c mice to influenza virus hemagglutinin. *Proc. Natl. Acad. Sci. U.S.A.*, **81**, 3180–3184.
17. Rajewsky,K. (1996) Clonal selection and learning in the antibody system. *Nature*, **381**, 751–758.
18. Pavlov,Y.I., Rogozin,I.B., Galkin,A.P., Aksenova,A.Y., Hanaoka,F., Rada,C. and Kunkel,T.A. (2002) Correlation of somatic hypermutation specificity and A-T base pair substitution errors by DNA polymerase eta during copying of a mouse immunoglobulin kappa light chain transgene. *Proc. Natl. Acad. Sci. U.S.A.*, **99**, 9954–9959.
19. Kunik,V., Ashkenazi,S. and Ofran,Y. (2012) Paratome: an online tool for systematic identification of antigen-binding regions in antibodies based on sequence or structure. *Nucleic Acids Res.*, **40**, W521–W524.
20. MacCarthy,T., Kalis,S.L., Roa,S., Pham,P., Goodman,M.F., Scharff,M.D. and Bergman,A. (2009) V-region mutation in vitro, in vivo, and in silico reveal the importance of the enzymatic properties of AID and the sequence environment. *Proc. Natl. Acad. Sci. U.S.A.*, **106**, 8629–8634.
21. Pham,P., Malik,S., Mak,C., Calabrese,P.C., Roeder,R.G. and Goodman,M.F. (2019) AID-RNA polymerase II transcription-dependent deamination of IgV DNA. *Nucleic Acids Res.*, **47**, 10815–10829.
22. Wei,L., Chahwan,R., Wang,S., Wang,X., Pham,P.T., Goodman,M.F., Bergman,A., Scharff,M.D. and MacCarthy,T. (2015) Overlapping hotspots in CDRs are critical sites for V region diversification. *Proc. Natl. Acad. Sci. U.S.A.*, **112**, E728–E737.
23. Ohm-Laursen,L. and Barington,T. (2007) Analysis of 6912 unselected somatic hypermutations in human VDJ rearrangements reveals lack of strand specificity and correlation between phase II substitution rates and distance to the nearest 3′ activation-induced cytidine deaminase target. *J. Immunol.*, **178**, 4322–4334.
24. Rada,C., Di Noia,J.M. and Neuberger,M.S. (2004) Mismatch recognition and uracil excision provide complementary paths to both Ig switching and the A/T-focused phase of somatic mutation. *Mol. Cell*, **16**, 163–171.
25. Low,N.M., Holliger,P.H. and Winter,G. (1996) Mimicking somatic hypermutation: affinity maturation of antibodies displayed on bacteriophage using a bacterial mutator strain. *J. Mol. Biol.*, **260**, 359–368.
26. Martineau,P. (2002) Error-prone polymerase chain reaction for modification of scFvs. *Methods Mol. Biol.*, **178**, 287–294.
27. Irving,R.A., Kortt,A.A. and Hudson,P.J. (1996) Affinity maturation of recombinant antibodies using E. coli mutator cells. *Immunotechnology*, **2**, 127–143.
28. Chowdhury,P.S. and Pastan,I. (1999) Improving antibody affinity by mimicking somatic hypermutation in vitro. *Nat. Biotechnol.*, **17**, 568–572.
29. Ahmad,Z.A., Yeap,S.K., Ali,A.M., Ho,W.Y., Alitheen,N.B. and Hamid,M. (2012) scFv antibody: principles and clinical application. *Clin. Dev. Immunol.*, **2012**, 980250.
30. Hassanzadeh-Ghassabeh,G., Devoogdt,N., De Pauw,P., Vincke,C. and Muyldermans,S. (2013) Nanobodies and their potential applications. *Nanomedicine (Lond)*, **8**, 1013–1026.
31. Thomas,W.D. and Smith,G.P. (2010) The case for trypsin release of affinity-selected phages. *BioTechniques*, **49**, 651–654.
32. Wu,F., Yang,L., Hang,K., Laursen,M., Wu,L., Han,G.W., Ren,Q., Roed,N.K., Lin,G., Hanson,M.A. *et al.* (2020) Full-length human GLP-1 receptor structure without orthosteric ligands. *Nat. Commun.*, **11**, 1272.
33. Pham,P., Afif,S.A., Shimoda,M., Maeda,K., Sakaguchi,N., Pedersen,L.C. and Goodman,M.F. (2016) Structural analysis of the activation-induced deoxycytidine deaminase required in immunoglobulin diversification. *DNA Repair (Amst.)*, **43**, 48–56.
34. Hust,M., Frenzel,A., Meyer,T., Schirrmann,T. and Dubel,S. (2012) Construction of human naive antibody gene libraries. *Methods Mol. Biol.*, **907**, 85–107.
35. Sebaugh,J.L. (2011) Guidelines for accurate EC50/IC50 estimation. *Pharm. Stat.*, **10**, 128–134.
36. Lippoldt,E.K., Elmes,R.R., McCoy,D.D., Knowlton,W.M. and McKemy,D.D. (2013) Artemin, a glial cell line-derived neurotrophic factor family member, induces TRPM8-dependent cold pain. *J. Neurosci.*, **33**, 12543–12552.
37. Lippoldt,E.K., Ongun,S., Kusaka,G.K. and McKemy,D.D. (2016) Inflammatory and neuropathic cold allodynia are selectively mediated by the neurotrophic factor receptor GFRalpha3. *Proc. Natl. Acad. Sci. U.S.A.*, **113**, 4506–4511.
38. National Research Council (U.S.) Committee for the Update of the Guide for the Care and Use of Laboratory Animals. Institute for Laboratory Animal Research (U.S.) and National Academies Press (U.S.) (2011) 8th edn., National Academy Press, Washington, D.C., p. 247.
39. Brezinschek,H.P., Brezinschek,R.I. and Lipsky,P.E. (1995) Analysis of the heavy chain repertoire of human peripheral B cells using single-cell polymerase chain reaction. *J. Immunol.*, **155**, 190–202.
40. Dal-Bo,M., Del Giudice,I., Bomben,R., Capello,D., Bertoni,F., Forconi,F., Laurenti,L., Rossi,D., Zucchetto,A., Pozzato,G. *et al.* (2011) B-cell receptor, clinical course and prognosis in chronic lymphocytic leukaemia: the growing saga of the IGHV3 subgroup gene usage. *Br. J. Haematol.*, **153**, 3–14.
41. Pham,P., Calabrese,P., Park,S.J. and Goodman,M.F. (2011) Analysis of a single-stranded DNA-scanning process in which activation-induced deoxycytidine deaminase (AID) deaminates C to U haphazardly and inefficiently to ensure mutational diversity. *J. Biol. Chem.*, **286**, 24931–24942.
42. Rogozin,I.B., Pavlov,Y.I., Bebenek,K., Matsuda,T. and Kunkel,T.A. (2001) Somatic mutation hotspots correlate with DNA polymerase eta error spectrum. *Nat. Immunol.*, **2**, 530–536.

43. Tang,C., Bagnara,D., Chiorazzi,N., Scharff,M.D. and MacCarthy,T. (2020) AID Overlapping and poleta hotspots are key features of evolutionary variation within the human antibody heavy chain (IGHV) genes. *Front. Immunol.*, **11**, 788.

44. Goodman,M.F., Scharff,M.D. and Romesberg,F.E. (2007) AID-initiated purposeful mutations in immunoglobulin genes. *Adv. Immunol.*, **94**, 127–155.

45. Muyldermans,S. (2013) Nanobodies: natural single-domain antibodies. *Annu. Rev. Biochem.*, **82**, 775–797.

46. Nauck,M.A., Kleine,N., Orskov,C., Holst,J.J., Willms,B. and Creutzfeldt,W. (1993) Normalization of fasting hyperglycaemia by exogenous glucagon-like peptide 1 (7-36 amide) in type 2 (non-insulin-dependent) diabetic patients. *Diabetologia*, **36**, 741–744.

47. Coopman,K., Huang,Y., Johnston,N., Bradley,S.J., Wilkinson,G.F. and Willars,G.B. (2010) Comparative effects of the endogenous agonist glucagon-like peptide-1 (GLP-1)-(7-36) amide and the small-molecule ago-allosteric agent "compound 2" at the GLP-1 receptor. *J. Pharmacol. Exp. Ther.*, **334**, 795–808.

48. Seierstad,M. and Breitenbucher,J.G. (2008) Discovery and development of fatty acid amide hydrolase (FAAH) inhibitors. *J. Med. Chem.*, **51**, 7327–7343.

49. O'Brien,M. and McDougall,J.J. (2018) Cannabis and joints: scientific evidence for the alleviation of osteoarthritis pain by cannabinoids. *Curr. Opin. Pharmacol.*, **40**, 104–109.

50. Ahn,K., Johnson,D.S., Mileni,M., Beidler,D., Long,J.Z., McKinney,M.K., Weerapana,E., Sadagopan,N., Liimatta,M., Smith,S.E. *et al.* (2009) Discovery and characterization of a highly selective FAAH inhibitor that reduces inflammatory pain. *Chem. Biol.*, **16**, 411–420.

51. Bransteitter,R., Pham,P., Calabrese,P. and Goodman,M.F. (2004) Biochemical analysis of hypermutational targeting by wild type and mutant activation-induced cytidine deaminase. *J. Biol. Chem.*, **279**, 51612–51621.

52. Rogozin,I.B. and Kolchanov,N.A. (1992) Somatic hypermutagenesis in immunoglobulin genes. II. Influence of neighbouring base sequences on mutagenesis. *Biochim. Biophys. Acta*, **1171**, 11–18.

53. Di Noia,J. and Neuberger,M.S. (2002) Altering the pathway of immunoglobulin hypermutation by inhibiting uracil-DNA glycosylase. *Nature*, **419**, 43–48.

54. Bruggemann,M., Osborn,M.J., Ma,B., Hayre,J., Avis,S., Lundstrom,B. and Buelow,R. (2015) Human antibody production in transgenic animals. *Arch. Immunol. Ther. Exp. (Warsz.)*, **63**, 101–108.

55. Nelson,A.L., Dhimolea,E. and Reichert,J.M. (2010) Development trends for human monoclonal antibody therapeutics. *Nat. Rev. Drug Discov.*, **9**, 767–774.

56. Marasco,W.A. and Sui,J. (2007) The growth and potential of human antiviral monoclonal antibody therapeutics. *Nat. Biotechnol.*, **25**, 1421–1434.

57. Persson,H., Kirik,U., Thornqvist,L., Greiff,L., Levander,F. and Ohlin,M. (2018) In vitro evolution of antibodies inspired by in vivo evolution. *Front. Immunol.*, **9**, 1391.

58. Zhang,D., Chen,C.F., Zhao,B.B., Gong,L.L., Jin,W.J., Liu,J.J., Wang,J.F., Wang,T.T., Yuan,X.H. and He,Y.W. (2013) A novel antibody humanization method based on epitopes scanning and molecular dynamics simulation. *PLoS One*, **8**, e80636.

59. Fujii,I. (2004) Antibody affinity maturation by random mutagenesis. *Methods Mol. Biol.*, **248**, 345–359.

60. Lou,J. and Marks,J.D. (2010) In: *Antibody Engineering*. Springer, pp.377–396.

61. Tiller,K.E., Chowdhury,R., Li,T., Ludwig,S.D., Sen,S., Maranas,C.D. and Tessier,P.M. (2017) Facile affinity maturation of antibody variable domains using natural diversity mutagenesis. *Front. Immunol.*, **8**, 986.

62. Pappas,L., Foglierini,M., Piccoli,L., Kallewaard,N.L., Turrini,F., Silacci,C., Fernandez-Rodriguez,B., Agatic,G., Giacchetto-Sasselli,I., Pellicciotta,G. *et al.* (2014) Rapid development of broadly influenza neutralizing antibodies through redundant mutations. *Nature*, **516**, 418–422.

63. Sidhu,S.S. and Fellouse,F.A. (2006) Synthetic therapeutic antibodies. *Nat. Chem. Biol.*, **2**, 682–688.